

Analysis of Charmless Two-body B decays in Factorization Assisted Topological Amplitude Approach

Si-Hong Zhou^a, Qi-An Zhang^a, Wei-Ran Lyu^b and Cai-Dian Lü^a

^a *Institute of High Energy Physics,*

YuQuanLu 19B, Beijing 100049, China;

School of Physics, University of Chinese Academy of Sciences,

YuQuanLu 19A, Beijing 100049, China; and

^b *Physics Department, Renmin University of China,*

ZhongGuanCun St. 59, Beijing 100872, China

(Dated: August 10, 2016)

Abstract

We analyze charmless two-body non-leptonic B decays $B \rightarrow PP, PV$ under the framework of factorization assisted topological amplitude approach, where $P(V)$ denotes a light pseudoscalar (vector) meson. Compared with the conventional flavor diagram approach, we consider flavor $SU(3)$ breaking effect assisted by factorization hypothesis for topological diagram amplitudes of different decay modes, factorizing out the corresponding decay constants and form factors. The non-perturbative parameters of topology diagram magnitudes χ and strong phase ϕ are universal that can be extracted by χ^2 fit from current abundant experimental data of charmless B decays. The number of free parameters and the χ^2 per degree of freedom are both reduced comparing with previous analysis. With these best fitted parameters, we predict branching fractions and CP asymmetry parameters of nearly 100 $B_{u,d}$ and B_s decay modes. The long-standing $\pi\pi$ and πK - CP puzzles are resolved simultaneously.

PACS numbers:

I. INTRODUCTION

Charmless two-body non-leptonic B decays are of importance for testing the standard model(SM). They can be used to study CP violation via the interference of tree and penguin contributions. They are also sensitive to signals of new physics that would change the small loop effects from penguin diagrams. With regards to them, the BarBar and Bell experiments at the e^+e^- B -factories[1] and LHCb experiment at the Large Hadron Collider(LHC)[2] have made great efforts in studying B decays information in the past decades. Numerous data of branching fractions and CP asymmetries of $B \rightarrow PP, PV$ decays, where $P(V)$ denotes a light pseudoscalar (vector) meson, have been measured. In particular, running at higher sensitivities and statistics, several B_s decay channels have been observed in LHCb experiment. Such abundant experimental data have made it possible to extract non-perturbative parameters of hadronic decay amplitudes and to test theoretical calculations of $B \rightarrow PP, PV$ decays.

In the theoretical side, as the non-leptonic B decays include hadronic decay amplitudes, it requires complicated study of non-perturbative strong QCD dynamics. Furthermore, the charmless B decays not only involve tree topologies but also have penguin loop diagrams that made the theoretical calculations more complex. The measured large direct CP violation in charmless B decays indicates the existence of large strong phases, which mainly come from non-perturbative QCD dynamics. In the heavy b quark mass limit, we can factorize the perturbative calculable part from the non-perturbative hadronic matrix elements. The naive factorization approach [3] was first invented to estimate the hadronic decay amplitudes, where they were factorized into the product of perturbative hard kernels (local four quark operators) and non-perturbative objects such as B to light form factors and decay constants of light pseudoscalar/vector mesons. Then it was later improved to the generalized factorization approach[4]. Based on the leading order power expansion of Λ_{QCD}/m_b , where Λ_{QCD} represents the typical non-perturbative QCD hadronic scale, m_b is b quark mass, the QCD factorization (QCDF) [5], the perturbative QCD (PQCD)[6], and the soft-collinear effective theory (SCET)[7] have been developed recently. Great theoretical progress have been made in these perturbative QCD approaches. However, it is impossible to calculate to all order of power expansions, thus some strong QCD dynamics information would be lost in these perturbative approaches. With the very high precision of experimental data, the leading-

order theoretical calculation of Λ_{QCD}/m_b expansion is not enough. For example, QCDF [8] need to include a large penguin annihilation contribution (as free parameter) to enhance the branching fractions and direct CP asymmetry of penguin-dominated charmless B decays. The same puzzle also appeared in SCET [9], where the penguin annihilation contribution in QCDF is replaced by the power suppressed (but with larger numerical contribution than the leading terms) nonperturbative charming penguin effect. All these power corrections are not able to calculate perturbatively but need to be fitted from experiments. There are also some experimental puzzles to be solved for those perturbative approaches. The perturbative calculation predict the same sign of direct CP asymmetry in $B^\pm \rightarrow \pi^0 K^\pm$ and in $B^0 \rightarrow \pi^\mp K^\pm$ decays, which is conflict with experimental data. The calculated branching ratio of $B^0 \rightarrow \pi^0 \pi^0$ in perturbative approaches is several times smaller than the measured one. These long-standing puzzles are sensitive to the non-factorizable color suppressed emission diagram. Although some soft and sub-leading effects were taken into account in QCDF [8] and PQCD [10], the $B \rightarrow \pi\pi$ puzzle was still left in the conventional factorization theorem. Recently, an additional Glauber phase is introduced to solve this puzzle [11].

Unlike the above mentioned perturbative approaches, some model-independent approaches were introduced to analyze the charmless B decays, such as global $SU(3)/U(3)$ flavor symmetry analysis [12] and flavor topological diagram approach [13, 14]. They do not apply factorization in QCD, leaving all perturbative or non-perturbative QCD effects extracted from experimental data. In [12], they related relevant decay amplitudes using $SU(3)/U(3)$ group decomposition and then extract them from experimental data. For the flavor topological diagram approach, they group different contributions according to the electroweak topological diagram, since electroweak interaction naturally factorize from QCD interaction. Each topological diagram amplitude including all strong interactions with strong phase are to be extracted from experimental data. However, in order to reduce the number of free parameters, it needs to apply the flavor $SU(3)$ symmetry to relate topological diagram parameters of different decay modes. In fact, the flavor $SU(3)$ symmetry is broken. Nowadays, $SU(3)$ breaking effect have to be considered to compare the theoretical results with the precise experimental data. It is also observed in the flavor topological diagram analysis that there are large differences among the three types of $B \rightarrow PP$, $B \rightarrow PV$ and $B \rightarrow VP$ decays due to different pseudoscalar and vector final states. Therefore, they have to fit three different sets of parameters for the three types of B decays respectively [14].

There are too many parameters to be fitted, its prediction power was reduced.

In view of the above complexity and incompleteness in power correction of factorization approaches and the limitation of the conventional flavor topological diagram approach, a new method called factorization-assisted-topological-amplitude (FAT) approach was proposed in studying the two-body hadronic decays of D mesons [15, 16]. Aiming to include all non-factorizable/non-perturbative QCD contributions compared to factorization approaches, it adopts the formalism of flavor topological diagram approach. However, different from the conventional flavor topological diagram approach, it had included $SU(3)$ breaking effect in each flavor topological diagram assisted by factorization hypothesis. The FAT approach applied in D mesons decays [15, 16] was in great success to resolve the long-standing puzzle from the large difference of $D^0 \rightarrow \pi^+\pi^-$ and $D^0 \rightarrow K^+K^-$ branching fractions, due to large $SU(3)$ breaking effects. It also predicted 0.1% of direct CP asymmetry difference between these two decay channels, later confirmed by the LHCb experiment [17]. With an intermediate charm quark scale, the two-body charmed meson decays of B meson also encounter large $SU(3)$ breaking effects [18]. With only 4 parameters fitted from 31 experimental observations, we predict 120 decay modes, some of which are tested by the available experimental data [18].

In this work, we will analyze the charmless $B \rightarrow PP, PV$ decays in the FAT approach. Being different from the two-body charmed B meson decays with only tree topologies, penguin topological diagrams enhanced by CKM matrix elements will contribute to these charmless B meson decays. These loop effect will be more complicated than the calculation to tree level diagrams. More theoretical parameters are needed to describe these penguin topological amplitudes and more experimental observables, such as CP asymmetry parameters. Specifically, including penguin topological contributions, we will fit 14 parameters from 37 experimental measured branching fractions and 11 CP asymmetry parameters of $B \rightarrow PP$ and $B \rightarrow PV$ decays. The number of free parameters is significantly reduced from the previous topological diagram approach with much less χ^2 per degree of freedom. The long-standing $B \rightarrow \pi\pi$ puzzle and $B \rightarrow \pi K$ CP puzzle are resolved consistently.

In Sec.II, we parameterize the tree and penguin topological amplitudes of charmless $B \rightarrow PP, PV$ decays in the FAT approach. The numerical results and discussions are presented in Sec.III. Sec.IV is the conclusion.

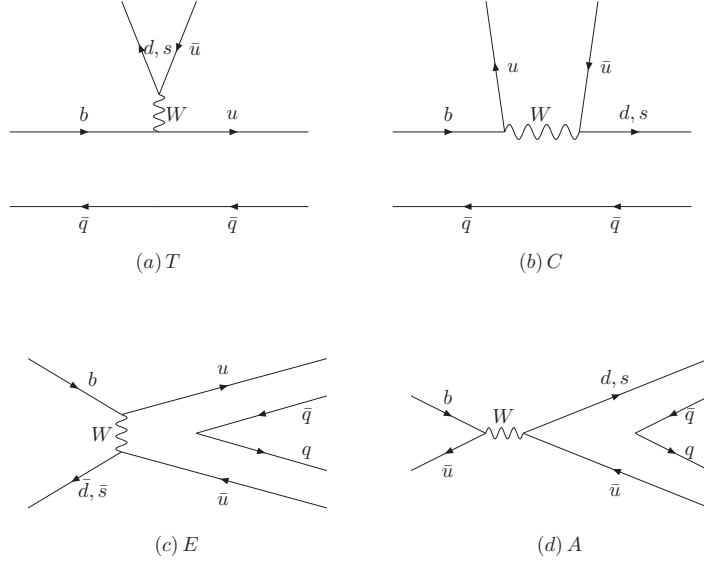


FIG. 1: Topological tree diagrams contributing to $B \rightarrow PP$ and $B \rightarrow PV$ decays: (a) the color-favored tree emission diagram, T ; (b) the color-suppressed tree emission diagram, C ; (c) the W -exchange diagram, E and (d) the W -annihilation diagram, A .

II. FACTORIZATION OF DECAY AMPLITUDES FOR DIFFERENT TOPOLOGICAL DIAGRAMS

The two body charmless B decays are flavor changing weak decays. They are induced by the quark level diagrams classified by leading order (tree diagram) and 1-loop level (penguin diagram) weak interactions. For different B decay final states, the tree level weak decay diagram can contribute via different orientations: the so-called color-favored tree emission diagram T , color-suppressed tree emission diagram C , W -exchange tree diagrams E and W annihilation tree diagrams A , which are shown in Fig.1, respectively. These tree level diagrams have already been studied in the previous D meson decays [15, 16] and charmed meson final state B decays [18]. Similarly, the 1-loop penguin diagram can also be classified as 5-types: color-favored QCD penguin emission diagram P , color-suppressed QCD penguin emission diagram P_C , W -annihilation penguin diagram P_A , the W penguin exchange diagram P_E and electro-weak penguin emission diagram P_{EW} , shown in Fig.2.

In the QCD factorization approaches, one try to calculate the QCD corrections to the specific weak diagrams or effective four quark operators order by order. The decay amplitude

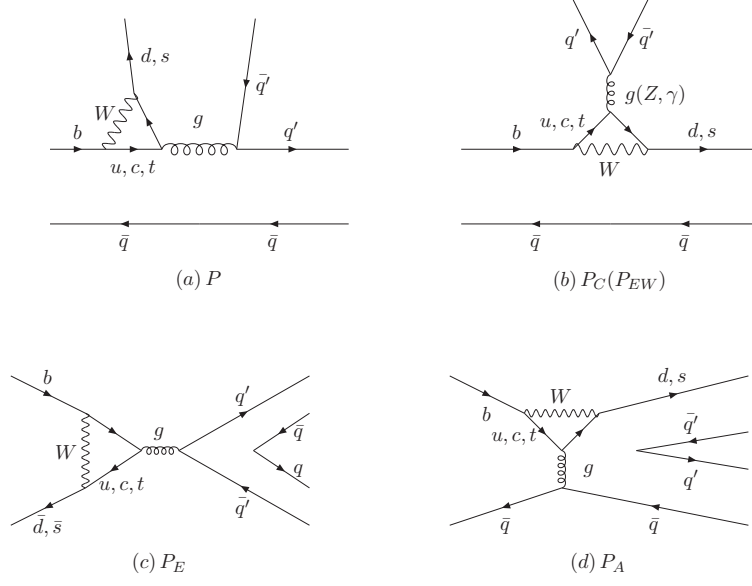


FIG. 2: Topological penguin diagrams contributing to $B \rightarrow PP$ and $B \rightarrow PV$ decays: (a) the color-favored QCD-penguin diagram, P ; (b) the flavor-singlet QCD-penguin diagram, P_C and EW-penguin diagram P_{EW} ; (c) the exchange type QCD-penguin diagram, P_E and (d) the QCD-penguin annihilation diagram, P_A .

for each decay is calculated in the factorization framework by the heavy quark expansion. In this work, to avoid the dependence of specific factorization approach, we extract the two-body hadronic weak decay amplitude of different topological diagram from the experimental data by the χ^2 fit. Therefore all strong interaction effects, the factorization and non-factorization contributions, perturbative and non-perturbative QCD corrections are all determined by experimental measurements. This is the idea of conventional topological diagram approach [14]. In order to have predictive power, one has to assume the flavor $SU(3)$ symmetry, reducing the number of independent parameters. The precision of this topological diagram approach is then limited to the order of $SU(3)$ breaking. In the FAT approach, we will try to recover the $SU(3)$ breaking effects, further reducing the number of free parameters by fitting all the decay channels.

Let's start from tree amplitudes shown in Fig.1. In the conventional topological diagram approach, the color favored tree amplitude (T) is tuned to be a real number, with 6 parameters (magnitudes and phases) for three other amplitudes. However, these 7 parameters have

to be tripled for $B \rightarrow PP$, $B \rightarrow PV$ and $B \rightarrow VP$ decays, since there is a non-negligible difference between pseudo-scalar and vector mesons. In this work, we will try to parametrize these three kinds of decays together. The color-favored T topology shown in Fig.1(a) is proved factorization to all orders of α_s expansion in QCD factorization, perturbative QCD, and soft-collinear-effective theory. Their numerical results also agree to each other in different approaches. Thus, to reduce one free parameter, we will just use their theoretical results, not fitting from the experiments:

$$T^{P_1 P_2} = i \frac{G_F}{\sqrt{2}} V_{ub} V_{uq'} a_1(\mu) f_{P_2} (m_B^2 - m_{P_1}^2) F_0^{BP_1}(m_{P_2}^2), \quad (1)$$

$$T^{PV} = \sqrt{2} G_F V_{ub} V_{uq'} a_1(\mu) f_V m_V F_1^{B-P}(m_V^2) (\varepsilon_V^* \cdot p_B), \quad (2)$$

$$T^{VP} = \sqrt{2} G_F V_{ub} V_{uq'} a_1(\mu) f_P m_V A_0^{B-V}(m_P^2) (\varepsilon_V^* \cdot p_B), \quad (3)$$

where the superscript of $T^{P_1 P_2}$ denote the final mesons are two pseudoscalar mesons, $T^{PV(VP)}$ for recoiling mesons are pseudoscalar meson (vector meson). $a_1(\mu)$ is the effective Wilson coefficient from short distance QCD corrections, where the factorization scale μ is insensitive to different final state mesons. Therefore we can choose it within a certain range arbitrarily and set it at the point $\mu = m_b/2 = 2.1\text{GeV}$. $a_1(\mu)$ at this scale is 1.05. $f_{P_2}(f_P)$ and f_V are the decay constants of emissive pseudoscalar meson and vector meson, respectively. $F_0^{BP_1}$ (F_1^{B-P}) and A_0^{B-V} are the form factors of $B \rightarrow P$ and $B \rightarrow V$ transitions, respectively. ε_V^* is the polarization vector of vector meson and p_B is the 4-momentum of B meson.

For the color suppressed C topology, dominated by non-factorization contributions, it is least-understood by us although having been calculated up to next-to-leading order in the factorization methods. The next-to-leading order corrections in factorization framework could not resolve the $\pi\pi$ and πK puzzles strongly sensitive to this C topology contribution. A large C contribution with large strong phase (mostly non-perturbative) can resolve the so called πK puzzle. However, it is not possible to explain the $\pi\pi$ puzzle: theoretically $Br(B^0 \rightarrow \pi^0 \pi^0) < Br(B^0 \rightarrow \pi^0 \rho^0) < Br(B^0 \rightarrow \rho^0 \rho^0)$, but experimentally it is in the inverse order. In the conventional topological diagram approach [14], the authors introduced two parameters (amplitude and phase) in the $B \rightarrow PP$ modes and another four parameters in the $B \rightarrow PV, VP$ modes for this diagram to be fitted from experimental data. To our knowledge, this inverse order can be understood only in the formalism of Glauber gluons introduced in ref.[11], where extra phase was introduced for the pseudo-scalar meson (Goldstone boson) emission diagram. Inspired by these studies, We parameterize the C diagram magnitude

and associate phase as χ^C and $e^{i\phi^C}$ in $B \rightarrow PP$, VP decays and $\chi^{C'} e^{i\phi^{C'}}$ in $B \rightarrow PV$, respectively to distinguish cases in which the emissive meson is pseudo-scalar or vector:

$$\begin{aligned} C^{P_1 P_2} &= i \frac{G_F}{\sqrt{2}} V_{ub} V_{uq'} \chi^C e^{i\phi^C} f_{p_2} (m_B^2 - m_{p_1}^2) F_0^{BP_1}(m_{p_2}^2), \\ C^{PV} &= \sqrt{2} G_F V_{ub} V_{uq'} \chi^{C'} e^{i\phi^{C'}} f_V m_V F_1^{B-P}(m_V^2) (\varepsilon_V^* \cdot p_B), \\ C^{VP} &= \sqrt{2} G_F V_{ub} V_{uq'} \chi^C e^{i\phi^C} f_P m_V A_0^{B-V}(m_P^2) (\varepsilon_V^* \cdot p_B), \end{aligned} \quad (4)$$

where the decay constants and form factors f_P , f_V , $F_0^{BP_1}$, F_1^{B-P} and A_0^{B-V} characterizing the $SU(3)$ breaking effects are factorized out.

The W-exchange E topology is non-factorization in QCD factorization approach. It is expected smaller than emission diagram due to helicity suppression. We use χ^E , $e^{i\phi^E}$ to represent the magnitude and its strong phase for all decay modes:

$$\begin{aligned} E^{P_1 P_2} &= i \frac{G_F}{\sqrt{2}} V_{ub} V_{uq'} \chi^E e^{i\phi^E} f_B m_B^2 \left(\frac{f_{p_1} f_{p_2}}{f_\pi^2} \right), \\ E^{PV, VP} &= \sqrt{2} G_F V_{ub} V_{uq'} \chi^E e^{i\phi^E} (\mu) f_B m_V \left(\frac{f_P f_V}{f_\pi^2} \right) (\varepsilon_V^* \cdot p_B), \end{aligned} \quad (5)$$

Considering flavor $SU(3)$ breaking effects, we multiply decay constants of three mesons $f_B, f_{p_1} (f_P)$ and $f_{p_2} (f_V)$ in each amplitude. In order to make parameters χ^E and $e^{i\phi^E}$ dimensionless, a normalization factor f_π^2 is introduced. Actually, dimensionless parameters χ^E , $e^{i\phi^E}$ are defined from $B \rightarrow \pi\pi$ decays. Other processes are related by different decay constant factors $\frac{f_{p_2} f_{p_1} (f_P f_V)}{f_\pi f_\pi}$. The last diagram in Fig.1(d) is the so called W-annihilation topology. As discussed in ref.[14], its contribution is negligible. We will also ignore it in this paper.

The penguin topological diagrams are grouped into QCD penguin and electro-weak penguin (EW penguin) topologies. In terms of QCD penguin diagram amplitude, we consider all contributions from every topological diagram in Fig.2, where topology P contributes most. The leading contribution from topology P diagram is similar to the color favored tree diagram T , which is proved factorization in various QCD-inspired approaches, such as QCD factorization [8], perturbative QCD [6] and soft-collinear effective theory [19]. They give very similar numerical results proportional to the Wilson coefficient a_4 , related to the QCD penguin operators O_3, O_4 . Therefore, in the same spirit of T diagram, we will not fit this contribution from the experimental data, but predict its contribution from QCD calculations for all the three type of $B \rightarrow PP$, $B \rightarrow VP$ and $B \rightarrow PV$ decays. This is not the whole story.

All these approaches predict large extra contribution in this topology related to the effective four-quark operators O_5 , O_6 , which is also called the “chiral enhanced” penguin contributions. Since this chiral enhancement only contributes to the pseudo-scalar meson (Goldstone boson) emission diagram, we will include it only in $B \rightarrow PP$ and $B \rightarrow VP$ decays, which can be parameterize as $r_\chi \chi^P$, $e^{i\phi^P}$ in Eq.(6) with r_χ the chiral factor of pseudo-scalar meson. The decay amplitude for the penguin diagram P is then parameterized with only two free parameters for all the three categories of $B \rightarrow PP$, $B \rightarrow VP$ and $B \rightarrow PV$ decays, as

$$\begin{aligned} P^{PP} &= -i \frac{G_F}{\sqrt{2}} V_{tb} V_{tq'}^* \left[a_4(\mu) + \chi^P e^{i\phi^P} r_\chi \right] f_{p_2} (m_B^2 - m_{p_1}^2) F_0^{BP_1}(m_{p_2}^2), \\ P^{PV} &= -\sqrt{2} G_F V_{tb} V_{tq'}^* a_4(\mu) f_V m_V F_1^{B-P} m_V^2 (\varepsilon_V^* \cdot p_B), \\ P^{VP} &= -\sqrt{2} G_F V_{tb} V_{tq'}^* \left[a_4(\mu) - \chi^P e^{i\phi^P} r_\chi \right] f_P m_V A_0^{B-V}(m_P^2) (\varepsilon_V^* \cdot p_B). \end{aligned} \quad (6)$$

The so called penguin annihilation diagram P_A shown in Fig.2(d) was considered as a power correction to P , calculated perturbatively in PQCD approach [6], parameterized as ρ_A , ϕ_A in QCDF [8] and replaced by the long-distance charming penguins as A_{cc}^{PP} , A_{cc}^{PV} and A_{cc}^{VP} in $B \rightarrow PP$, $B \rightarrow VP$ and $B \rightarrow PV$ decays, respectively in SCET [19]. Numerically it is not small. However, if one read this diagram carefully, one can find that it is not distinguishable in weak interaction from the diagram P in Fig.2(a). The only difference between these two diagrams is the gluon exchange. Since all the QCD dynamics will be determined by χ^2 fit from the experimental data, we will not introduce more parameters for this diagram in $B \rightarrow PP$ and $B \rightarrow VP$ decays. The contribution of this diagram is already encoded in the parameter $r_\chi \chi^P$, $e^{i\phi^P}$ in Eq.(6) for diagram Fig.2(a). But for $B \rightarrow PV$ decays, we do need two parameters χ^{P_A} , $e^{i\phi^{P_A}}$ for penguin annihilation diagram P_A shown in Fig.2(d):

$$P_A^{PV} = -\sqrt{2} G_F V_{tb} V_{tq'}^* \chi^{P_A} e^{i\phi^{P_A}} f_B m_V \left(\frac{f_P f_V}{f_\pi^2} \right) (\varepsilon_V^* \cdot p_B). \quad (7)$$

The contribution from P_E diagram shown in Fig.2(c) is argued smaller than P_A diagram, which can be ignored reliably in decay modes not dominated by it such as measured $B^0 \rightarrow \pi^+ \pi^-$, $B^0 \rightarrow \pi^0 \pi^0$, $B^0 \rightarrow K^0 \bar{K}^0$ and $B^0 \rightarrow \pi^0 \rho^0$ decays. This P_E contribution actually is the dominant contribution for the recent measurement of $B_s \rightarrow \pi^+ \pi^-$ decay [21]

$$Br(B_s \rightarrow \pi^+ \pi^-) = (0.76 \pm 0.19) \times 10^{-6}. \quad (8)$$

We do not intend to use this single measurement to determine the contribution from this diagram P_E . Thus we have to ignore it for later discussion.

The flavor-singlet QCD penguin diagram P_C only contribute to the isospin singlet mesons η , η' , ω and ϕ . Anomaly related or not, there is also significant difference between these pseudo-scalar mesons and vector mesons. We distinguish them as χ^{P_C} , $e^{i\phi^{P_C}}$ for $B \rightarrow PP$ and $B \rightarrow VP$ decays and $\chi^{P'_C}$, $e^{i\phi^{P'_C}}$ for $B \rightarrow PV$ decays, respectively:

$$\begin{aligned} P_C^{PP} &= -i \frac{G_F}{\sqrt{2}} V_{tb} V_{tq}^* \chi^{P_C} e^{i\phi^{P_C}} f_{p_2} (m_B^2 - m_{p_1}^2) F_0^{BP_1}(m_{p_2}^2), \\ P_C^{PV} &= -\sqrt{2} G_F V_{tb} V_{tq}^* \chi^{P'_C} e^{i\phi^{P'_C}} f_V m_V F_1^{B-P}(m_V^2) (\varepsilon_V^* \cdot p_B), \\ P_C^{VP} &= -\sqrt{2} G_F V_{tb} V_{tq}^* \chi^{P_C} e^{i\phi^{P_C}} f_P m_V A_0^{B-V}(m_P^2) (\varepsilon_V^* \cdot p_B), \end{aligned} \quad (9)$$

The EW-penguin contribution is much smaller than QCD penguin diagram, as the coupling coefficient α_{em} is one order smaller than α_s . We only keep its largest contribution diagram shown in the second one of Fig.2, with gluon g replaced by Z or γ with respect to QCD penguin diagram. Although the topology of P_C diagram is quite similar to the P_{EW} topology, their contributions are different. They both contribute to the isospin singlet meson emission decays. But P_{EW} topology also contribute to the neutral isospin 1 meson emission decays. The topology of this diagram is very similar to the T diagram. Factorization can be approved without ambiguity. Without introducing new parameters, we evaluate it similar to T ,

$$\begin{aligned} P_{EW}^{PP} &= -i \frac{G_F}{\sqrt{2}} V_{tb} V_{tq}^* e_q \frac{3}{2} a_9(\mu) f_{p_2} (m_B^2 - m_{p_1}^2) F_0^{BP_1}(m_{p_2}^2), \\ P_{EW}^{PV} &= -\sqrt{2} G_F V_{tb} V_{tq}^* e_q \frac{3}{2} a_9(\mu) f_V m_V F_1^{B-P}(m_V^2) (\varepsilon_V^* \cdot p_B), \\ P_{EW}^{VP} &= -\sqrt{2} G_F V_{tb} V_{tq}^* e_q \frac{3}{2} a_9(\mu) f_P m_V A_0^{B-V}(m_P^2) (\varepsilon_V^* \cdot p_B), \end{aligned} \quad (10)$$

where $a_9(\mu)$ is the effective Wilson coefficient equal to -0.009 at scale $\mu = 2.1 \text{ GeV}$.

With all the decay amplitudes settled, the decay width for two-body charmless B decays is given by

$$\Gamma(B \rightarrow M_1 M_2) = \frac{p}{8\pi m_B^2} \sum_{pol} |\mathcal{A}|^2, \quad (11)$$

where M_1, M_2 represent either two pseudoscalar P_1, P_2 or one pseudoscalar P and one vector V in the final states. p is the 3 dimension momentum of either meson in the final state in the center-of-mass frame. The summation over the polarization states is for vector meson state. The corresponding branching fraction is

$$\mathcal{B}(B \rightarrow M_1 M_2) = \frac{\Gamma(B \rightarrow M_1 M_2) + \Gamma(\bar{B} \rightarrow \bar{M}_1 \bar{M}_2)}{2} \times \tau_B, \quad (12)$$

where τ_B is the B meson lifetime. The CP violation charge asymmetry of exclusive B^- and B^+ decay is defined as

$$\mathcal{A}_{cp} = \frac{\mathcal{B}(B^- \rightarrow \bar{M}_1 \bar{M}_2) - \mathcal{B}(B^+ \rightarrow M_1 M_2)}{\mathcal{B}(B^- \rightarrow \bar{M}_1 \bar{M}_2) + \mathcal{B}(B^+ \rightarrow M_1 M_2)}. \quad (13)$$

For the neutral $B_{(s)}$ mesons, there is a complication because of the $B_{(s)}^0 - \bar{B}_{(s)}^0$ mixing, if the decay product is a CP eigenstate. The CP asymmetry is time dependent:

$$\mathcal{A}_{cp}(t) = \mathcal{S}_f \sin(\Delta m_B t) - \mathcal{C}_f \cos(\Delta m_B t), \quad (14)$$

where Δm_B is the mass difference between the two mass eigenvalues of B mesons. $\mathcal{A}_{cp} \equiv -\mathcal{C}_f$ is the direct CP asymmetry and \mathcal{S}_f is the mixing induced CP asymmetry parameter, which are calculated as:

$$\begin{aligned} \mathcal{C}_f &= \frac{1 - |\lambda_f|^2}{1 + |\lambda_f|^2}, \\ \mathcal{S}_f &= \frac{2\text{Im}(\lambda_f)}{1 + |\lambda_f|^2}, \end{aligned} \quad (15)$$

where $\lambda_f = \frac{g}{p} \frac{\bar{A}_f}{A_f}$ and $\frac{g}{p} = \frac{V_{tb}^* V_{td}}{V_{tb} V_{td}^*}$ or $\left(\frac{V_{tb}^* V_{ts}}{V_{tb} V_{ts}^*}\right)$, which is the mixing parameter for $B_{(s)}^0 - \bar{B}_{(s)}^0$ mixing. A_f is the decay amplitude of $B^0 \rightarrow f_{CP}$ and \bar{A}_f is the amplitude of the CP -conjugate process.

If the decay product is not a CP eigenstate, the $B_{(s)}^0 - \bar{B}_{(s)}^0$ mixing will not result in a mixing induced CP asymmetry, but only a direct CP asymmetry like the B^\pm decays (for example $B^0 \rightarrow \pi^- K^+$). However, for the $\bar{B}^0 \rightarrow \pi^\pm \rho^\mp$, $\bar{B}^0 \rightarrow K_s K^{*0}(K^{*0})$, $\bar{B}_s \rightarrow K^\pm K^{*\mp}$ and $\bar{B}_s \rightarrow K_s K^{*0}(K^{*0})$ decay modes, the $B_{(s)}^0 - \bar{B}_{(s)}^0$ mixing still plays an important role, even if the final states are not CP eigenstates. The reason is that both $B_{(s)}^0$ and $\bar{B}_{(s)}^0$ meson can decay to the same final state. The CP asymmetry is time dependent with four equations [20]. There is a mismatch between theoretical and experimental variables. We adopt the convention of ref. [14], for example, the mixing-induced CP asymmetries S_{cp} for the $\bar{B}^0 \rightarrow \pi^\pm \rho^\mp$ shown as,

$$\begin{aligned} \mathcal{S}_{\bar{B}^0 \rightarrow \pi^+ \rho^-} &= \frac{2\text{Im}(\lambda_{\bar{B}^0 \rightarrow \pi^+ \rho^-})}{1 + |\lambda_{\bar{B}^0 \rightarrow \pi^+ \rho^-}|^2}, \\ \mathcal{S}_{\bar{B}^0 \rightarrow \pi^- \rho^+} &= \frac{2\text{Im}(\lambda_{\bar{B}^0 \rightarrow \pi^- \rho^+})}{1 + |\lambda_{\bar{B}^0 \rightarrow \pi^- \rho^+}|^2}, \end{aligned} \quad (16)$$

TABLE I: The decay constants of light pseudo-scalar mesons and vector mesons (in unit of MeV).

f_π	f_K	f_B	f_{B_s}	f_ρ	f_{K^*}	f_ω	f_ϕ
130	156	190	225	213	220	192	225

where

$$\begin{aligned}\lambda_{\bar{B}^0 \rightarrow \pi^+ \rho^-} &= \frac{q}{p} \frac{A(\bar{B}^0 \rightarrow \pi^+ \rho^-)}{A(B^0 \rightarrow \pi^- \rho^+)}, \\ \lambda_{\bar{B}^0 \rightarrow \pi^- \rho^+} &= \frac{q}{p} \frac{A(\bar{B}^0 \rightarrow \pi^- \rho^+)}{A(B^0 \rightarrow \pi^+ \rho^-)}.\end{aligned}\tag{17}$$

The definition of S_{cp} for the $\bar{B}^0 \rightarrow K_s K^{*0}(K^{*0})$, $\bar{B}_s \rightarrow K^\pm K^{*\mp}$ and $\bar{B}_s \rightarrow K_s K^{*0}(K^{*0})$ decays are similar with $\bar{B}^0 \rightarrow \pi^\pm \rho^\mp$.

III. NUMERICAL RESULTS AND DISCUSSIONS

A. Input parameters

The input parameters used in decay amplitudes mainly contain the CKM matrix elements, decay constants and transition form factors. We use the Wolfenstein parametrization for V_{CKM} with the Wolfenstein parameters obtained from [21]:

$$\lambda = 0.22537 \pm 0.00061, \quad A = 0.814_{-0.024}^{+0.023}$$

$$\bar{\rho} = 0.117 \pm 0.021, \quad \bar{\eta} = 0.353 \pm 0.013.$$

Table I represents the decay constants of light meson (P , V). The measured f_π and f_K are given in average by PDG [21]. The value of f_B, f_{B_s} and the decay constants of vector mesons not measured directly in experiments but can be got from several theoretical approaches, such as in Covariant light front approach [22] light-cone sum rules [23, 24], QCD sum rules [25–30], or lattice QCD [31–38]. We show only central values in Table I and keep 5% uncertainty, when estimate theoretical uncertainty of branching fractions and CP asymmetry parameters.

The transition form factors of B meson decays were calculated in various theoretical approaches, constitute quark model and light cone quark model [39–42], Covariant light

front approach(LFQM) [22, 43, 44], light-cone sum rules [24, 45–63], PQCD [64–72] and lattice QCD [73–75]. The central values of the transition form factors of B meson decays at $q^2=0$ are shown in Table II. The error bar of them are kept in 10%. This uncertainty of hadronic form factors is one of the major source of theoretical uncertainty in our calculation as shown in next section. For the q^2 dependence of the transition form factors, we use the dipole parametrization:

$$F_i(q^2) = \frac{F_i(0)}{1 - \alpha_1 \frac{q^2}{M_{\text{pole}}^2} + \alpha_2 \frac{q^4}{M_{\text{pole}}^4}}, \quad (18)$$

where F_i denotes F_0 , F_1 , and A_0 in this article, and M_{pole} is the mass of the corresponding pole state, such as $B_{(s)}$ for A_0 , and $B_{(s)}^*$ for $F_{0,1}$. α_1 and α_2 are the dipole parameters as shown in Table II. Since the values of $q^2=m_{P,V}^2$, where $m_{P,V}$ is the mass of emission meson in $B \rightarrow PP, PV$ decays, are small compared with the pole mass, this q^2 dependence will not affect our numerical results significantly.

For the η and η' meson in the final state of B decays, their decay constants and form factors are defined through $\eta - \eta'$ mixing,

$$\begin{pmatrix} \eta \\ \eta' \end{pmatrix} = \begin{pmatrix} \cos \phi & -\sin \phi \\ \sin \phi & \cos \phi \end{pmatrix} \begin{pmatrix} \eta_q \\ \eta_s \end{pmatrix}, \quad (19)$$

where η_q and η_s are defined by

$$\eta_q = \frac{1}{\sqrt{2}}(u\bar{u} + d\bar{d}), \quad \eta_s = s\bar{s}. \quad (20)$$

The mixing angle is measured to be $\phi = (40.4 \pm 0.6)^\circ$ by KLOE [76]. The flavor decay constants of η_q and η_s are $f_q = (1.07 \pm 0.02)f_\pi$ and $f_s = (1.34 \pm 0.06)f_\pi$ respectively [77, 78]. In a good approximation, we neglect the ω and ϕ mixing effect.

B. The χ^2 fit for theoretical parameters

After the usage of factorization theorem, the number of theoretical parameters to be fitted from experimental data is reduced. The 6 parameters for tree diagrams are: color suppressed tree diagram amplitude χ^C , $\chi^{C'}$ and their phases ϕ^C , $\phi^{C'}$; W-exchange diagram amplitude χ^E and its phase ϕ^E . The 8 parameters for penguin diagrams are: Chiral enhanced penguin amplitude χ^P and its phase ϕ^P ; flavor singlet penguin amplitude χ^{Pc} , $\chi^{P'c}$ and their phases ϕ^{Pc} , $\phi^{P'c}$ for the pseudo-scalar and vector meson emission, respectively; the penguin

TABLE II: The transition form factors of B meson decays at $q^2=0$ and dipole model parameters

	$F_0^{B \rightarrow \pi}$	$F_0^{B \rightarrow K}$	$F_0^{B_s \rightarrow K}$	$F_0^{B \rightarrow \eta_q}$	$F_0^{B_s \rightarrow \eta_s}$
$F(0)$	0.28	0.31	0.25	0.21	0.30
α_1	0.50	0.53	0.54	0.52	0.53
α_2	-0.13	-0.13	-0.15	0	0
	$F_1^{B \rightarrow \pi}$	$F_1^{B \rightarrow K}$	$F_1^{B_s \rightarrow K}$	$F_1^{B \rightarrow \eta_q}$	$F_1^{B_s \rightarrow \eta_s}$
$F(0)$	0.28	0.31	0.25	0.21	0.30
α_1	0.52	0.54	0.57	1.43	1.48
α_2	0.45	0.50	0.50	0.41	0.46
	$A_0^{B \rightarrow \rho}$	$A_0^{B \rightarrow \omega}$	$A_0^{B \rightarrow K^*}$	$A_0^{B_s \rightarrow K^*}$	$A_0^{B_s \rightarrow \phi}$
$A(0)$	0.36	0.32	0.39	0.33	0.40
α_1	1.56	1.60	1.51	1.74	1.73
α_2	0.17	0.22	0.14	0.47	0.41

annihilation amplitude χ^{P_A} and its phase ϕ^{P_A} for the vector meson emission only. Many of the charmless B decays channels have been experimentally measured [21]. But some of them are measured with very poor precision. In our χ^2 fit program, we will not use those data with less than 3σ significance. For the B_s meson decays, very few modes are measured, some of which are measured only by hadronic colliders such LHCb and CDF experiments. The precision of these B_s decays measurements rely heavily on other B decay channels measured by B factories. Thus the systematic uncertainty of them is correlated. We will not use the B_s decay data to avoid complications. After these considerations, we have 37 branching Ratios and 11 CP violation observations of $B_{u,d} \rightarrow PP, PV$ decays from the current experimental data, where the branching ratios of $B^0 \rightarrow \pi^+ \rho^-$ and $B^0 \rightarrow \pi^- \rho^+$ are derived from experimental data in ref.[14]. With these 48 data, we use the χ^2 fit method by Miniut program [79] to give the best-fitted parameters and the corresponding 1σ uncertainty

as:

$$\begin{aligned}
\chi^C &= 0.48 \pm 0.06, & \phi^C &= -1.58 \pm 0.08, \\
\chi^{C'} &= 0.42 \pm 0.16, & \phi^{C'} &= 1.59 \pm 0.17, \\
\chi^E &= 0.057 \pm 0.005, & \phi^E &= 2.71 \pm 0.13, \\
\chi^P &= 0.10 \pm 0.02, & \phi^P &= -0.61 \pm 0.02, \\
\chi^{P_C} &= 0.048 \pm 0.003, & \phi^{P_C} &= 1.56 \pm 0.08, \\
\chi^{P'_C} &= 0.039 \pm 0.003, & \phi^{P'_C} &= 0.68 \pm 0.08, \\
\chi^{P_A} &= 0.0059 \pm 0.0008, & \phi^{P_A} &= 1.51 \pm 0.09,
\end{aligned} \tag{21}$$

with $\chi^2/\text{d.o.f} = 45.2/34 = 1.3$. This χ^2 per degree of freedom is smaller than the conventional flavor diagram approach based on flavor $SU(3)$ symmetry[14]. In fact, they have much more parameters [14] than in our work. From eq.(21), one can see that the color suppressed tree diagram amplitude χ^C and $\chi^{C'}$ have similar size but their phases ϕ^C and $\phi^{C'}$ differ significantly. Denoting the pseudo-scalar and vector meson emission, respectively, their differences agree with the Glauber gluon effects [11]. The similar differences are observed in the flavor singlet penguin amplitude χ^{P_C} , $\chi^{P'_C}$ and their phases ϕ^{P_C} , $\phi^{P'_C}$ for the pseudo-scalar and vector meson emission, respectively.

To show the relative size of every topological diagram in each decay mode, we take decay modes $B \rightarrow \pi\pi$ and $B \rightarrow \pi\rho$ to show the hierarchy of various tree and penguin topologies amplitude ($C(P_C)$ and $C'(P'_C)$ denote for the pseudo-scalar and vector meson emission respectively.), as follows:

$$T^{\pi\pi} : C^{\pi\pi} : E^{\pi\pi} : P^{\pi\pi} = 1 : 0.47 : 0.29 : 0.32 \tag{22}$$

$$T^{\rho\pi} : C'^{\pi\rho} : P^{\rho\pi} : P_{EW}^{\pi\rho} = 1 : 0.54 : 0.25 : 0.04 \tag{23}$$

$$T^{\pi\rho} : C^{\rho\pi} : P^{\rho\pi} : P_{EW}^{\rho\pi} = 1 : 0.36 : 0.19 : 0.03. \tag{24}$$

In these tree dominant decays, the relative importance of topological diagrams is easy to be reached:

$$T > C(C') > E \sim P > P_{EW}. \tag{25}$$

This is in agreement with those QCD inspired approaches. For $B \rightarrow \pi K$ and $B \rightarrow \pi K^*$

decays, we have

$$T^{\pi K} : C^{\pi K} : P^{\pi K} : P_{EW}^{\pi K} = 1 : 0.4 : 6.0 : 0.6 \quad (26)$$

$$T^{\pi K^*} : C^{K^* \pi} : P^{\pi K^*} : P_A^{\pi K^*} : P_{EW}^{K^* \pi} = 1 : 0.37 : 2.87 : 1.44 : 0.52. \quad (27)$$

In these penguin dominant decays, the relative importance of topological diagrams is also reached as:

$$P > P_A > T > P_{EW} > C. \quad (28)$$

It is interesting that the electroweak penguin contribution P_{EW} is even more larger than the color suppressed tree C . It is indeed not negligible. For $B \rightarrow \rho K$ decays, we have

$$T^{\rho K} : C'^{K \rho} : P^{\rho K} : P_{EW}^{K \rho} = 1 : 0.49 : 2.82 : 0.79. \quad (29)$$

In this channel, we have very similar contributions from each topology:

$$P > T > P_{EW} > C'. \quad (30)$$

Again, the electroweak penguin contribution P_{EW} is important.

As the P_C and P'_C only contribute to modes including flavor singlets meson $(\eta, \eta', \omega, \phi)$, the hierarchy including P_C and P'_C are represented as:

$$T^{\pi \eta} : C^{\pi \eta} : P^{\pi \eta} : P_C^{\pi \eta} : P_{EW}^{\pi \eta} = 1 : 0.50 : 0.57 : 0.06 : 0.03 \quad (31)$$

$$T^{\eta K} : C^{\eta K} : P^{\eta K} : P_C^{\eta K} : P_{EW}^{\eta K} = 1 : 0.45 : 3.39 : 1.10 : 0.52 \quad (32)$$

$$T^{\pi \omega} : C'^{\pi \omega} : P^{\pi \omega} : P_C^{\pi \omega} : P_A^{\pi \omega} : P_{EW}^{\pi \omega} = 1 : 0.54 : 0.21 : 0.26 : 0.10 : 0.02 \quad (33)$$

The flavor singlet penguin contribution P_C is important, as it is even larger than the color favored tree contribution T in ηK channel and it is at the similar size as penguin emission contribution P in $\pi \omega$ channel. The importance of this type of penguin contribution is recently emphasized [12].

C. Branching Ratios for the charmless B decays

After χ^2 fitting the parameters in Eq.(21), we get the numerical results of branching fractions for $\bar{B} \rightarrow PP$ decays shown in Table III and $\bar{B} \rightarrow PV$ decays in Table IV. Each branching fractions tables are divided into two parts: $\Delta S = 0$ transitions and $\Delta S = 1$

TABLE III: Branching fractions ($\times 10^{-6}$) of various $\bar{B} \rightarrow PP$ decay modes. We also show the experimental data [21] and results from conventional flavor diagram approach [14] for comparison.

Mode	Amplitudes	Exp	This work	Flavor diagram
$\pi^- \pi^0$	T, C, P_{EW}	$\star 5.5 \pm 0.4$	$5.08 \pm 0.39 \pm 1.02 \pm 0.02$	5.40 ± 0.79
$\pi^- \eta$	T, C, P, P_C, P_{EW}	$\star 4.02 \pm 0.27$	$4.13 \pm 0.25 \pm 0.64 \pm 0.01$	3.88 ± 0.39
$\pi^- \eta'$	T, C, P, P_C, P_{EW}	$\star 2.7 \pm 0.9$	$3.37 \pm 0.21 \pm 0.49 \pm 0.01$	5.59 ± 0.54
$\pi^+ \pi^-$	$T, E, (P_E), P$	$\star 5.12 \pm 0.19$	$5.15 \pm 0.36 \pm 1.31 \pm 0.14$	5.17 ± 1.03
$\pi^0 \pi^0$	$C, E, P, (P_E), P_{EW}$	$\star 1.91 \pm 0.22$	$1.94 \pm 0.30 \pm 0.28 \pm 0.05$	1.88 ± 0.42
$\pi^0 \eta$	$C, E, P_C, (P_E), P_{EW}$	< 1.5	$0.86 \pm 0.08 \pm 0.08 \pm 0.04$	0.56 ± 0.03
$\pi^0 \eta'$	$C, E, P_C, (P_E), P_{EW}$	1.2 ± 0.6	$0.87 \pm 0.08 \pm 0.10 \pm 0.03$	1.21 ± 0.16
$\eta \eta$	$C, E, P_C, (P_E), P_{EW}$	< 1.0	$0.44 \pm 0.09 \pm 0.08 \pm 0.005$	0.77 ± 0.12
$\eta \eta'$	$C, E, P_C, (P_E), P_{EW}$	< 1.2	$0.77 \pm 0.13 \pm 0.14 \pm 0.008$	1.99 ± 0.26
$\eta' \eta'$	$C, E, P_C, (P_E), P_{EW}$	< 1.7	$0.38 \pm 0.05 \pm 0.07 \pm 0.003$	1.60 ± 0.20
$K^- K^0$	P	$\star 1.31 \pm 0.17$	$1.32 \pm 0.04 \pm 0.26 \pm 0.01$	1.03 ± 0.02
$K^0 \bar{K}^0$	P	$\star 1.21 \pm 0.16$	$1.23 \pm 0.03 \pm 0.25 \pm 0.01$	0.89 ± 0.11
$\pi^- \bar{K}^0$	P	$\star 23.7 \pm 0.8$	$23.2 \pm 0.6 \pm 4.6 \pm 0.2$	23.53 ± 0.42
$\pi^0 K^-$	T, C, P, P_{EW}	$\star 12.9 \pm 0.5$	$12.8 \pm 0.32 \pm 2.35 \pm 0.10$	12.71 ± 1.05
ηK^-	T, C, P, P_C, P_{EW}	$\star 2.4 \pm 0.4$	$2.0 \pm 0.13 \pm 1.19 \pm 0.03$	1.93 ± 0.31
$\eta' K^-$	T, C, P, P_C, P_{EW}	$\star 70.6 \pm 2.5$	$70.1 \pm 4.7 \pm 11.3 \pm 0.22$	70.92 ± 8.54
$\pi^+ K^-$	T, P	$\star 19.6 \pm 0.5$	$19.8 \pm 0.54 \pm 4.0 \pm 0.2$	20.2 ± 0.39
$\pi^0 \bar{K}^0$	C, P, P_{EW}	$\star 9.9 \pm 0.5$	$8.96 \pm 0.26 \pm 1.96 \pm 0.09$	9.73 ± 0.82
$\eta \bar{K}^0$	C, P, P_C, P_{EW}	$\star 1.23 \pm 0.27$	$1.35 \pm 0.10 \pm 1.02 \pm 0.03$	1.49 ± 0.27
$\eta' \bar{K}^0$	C, P, P_C, P_{EW}	$\star 66 \pm 4$	$66.4 \pm 4.5 \pm 10.6 \pm 0.21$	66.51 ± 7.97

transitions. We also show the contributing topological amplitude symbols for each channel in these tables. For the theoretical uncertainties in the tables (apply also to the following tables), the first one is the statistical uncertainty from the χ^2 fitting by experimental data. The second one arise from the transition form factors which are set to be 10% uncertainties, and the third from decay constants. We can find that the dominant uncertainty for most

channels is from form factors, which need to be approved by theories and semi-leptonic B decay measurements. The experimental data are also shown in these tables to compare with theoretical predictions. Not all of the measurements are in a good accuracy. In our χ^2 fit program, we use those data only with more than 3σ signal significance that marked as a * in these tables. The rest can be considered as theoretical predictions, waiting for LHCb and other experiments to test.

From Table III and IV, one can easily find that $B(B^- \rightarrow \pi^- \pi^0)$ is twice smaller than $B(B^- \rightarrow \pi^0 \rho^-)$. These two modes receive similar contributions from the color favored tree diagram denoted by T , while all other contributions are suppressed. If not considering SU(3) breaking effects, one need two parameters to fit these two diagrams in ref.[14]. In our FAT approach, this can be easily explained by the fact that $f_\rho > f_\pi$, therefore we do not need any free parameter to be fitted from experimental data. Due to the difference between vector or pseudo-scalar emission in color suppressed tree diagram $\chi^{C'}$ and χ^C , especially the very larger strong phase difference, the $B(B^- \rightarrow \rho^- \pi^0)$ is a little different from $B(B^- \rightarrow \rho^0 \pi^-)$. Interestingly, for the penguin dominated B decays it is the inverse situation. The branching fractions of the penguin diagram P dominated decay modes $B^- \rightarrow \pi^- \bar{K}^0$, $B^- \rightarrow \pi^0 K^-$ and $\bar{B}^0 \rightarrow \pi^0 \bar{K}^0$ are larger than their corresponding ones of $B \rightarrow PV$ decays. This can be understood from eq.(6) that in addition to the factorizable amplitude of QCD penguin emission topology, there is a large chiral enhanced penguin contribution in $B \rightarrow PP$ modes; while no such contribution in $B \rightarrow PV$ modes and negative contribution in $B \rightarrow VP$ modes.

Similar to the conventional topological diagram approach [14], the long-standing puzzle of large $B^0 \rightarrow \pi^0 \pi^0$ branching fraction can be resolved well attributed to the appropriate magnitude and phase of C in FAT. Naive estimation indicates that $|C|/|T|$ is about 1/3 due to color suppressed factor. The χ^C are enhanced by large nonperturbative contribution such as final states interaction and re-scattering effects. Although some power corrections to them were parameterized in QCDF, PQCD and SCET as mentioned before, where the $\pi\pi$ puzzle was accommodated to some extent, it is not resolved completely in those factorization approaches. With a larger $B^0 \rightarrow \pi^0 \pi^0$ branching fraction, the $B^0 \rightarrow \pi^0 \rho^0$ and $B^0 \rightarrow \rho^0 \rho^0$ branching ratio will go easily much larger than the experimental data. Actually, only the Glauber phase factor [11], associated with the Goldstone boson π can resolve the $B \rightarrow \pi\pi$, $B \rightarrow \pi\rho$ and $B \rightarrow \rho\rho$ puzzles consistently. We predict these branching ratios correctly in Table III with not too large χ^C . $|T^{\pi\pi}| : |C^{\pi\pi}| = 1 : 0.47$ shown in Eq.(22) is not as large as

TABLE IV: Branching fractions ($\times 10^{-6}$) of various $\bar{B} \rightarrow PV$ decay modes. We also show the experimental data [21] and results from conventional flavor diagram approach [14] for comparison.

Mode	Amplitudes	Exp	This work	Flavor diagram
$\pi^- \rho^0$	T, C', P, P_A, P_{EW}	$\star 8.3 \pm 1.2$	$8.6 \pm 1.81 \pm 1.38 \pm 0.03$	7.59 ± 1.41
$\pi^- \omega$	$T, C', P, P'_C, P_A, P_{EW}$	$\star 6.9 \pm 0.5$	$6.78 \pm 1.46 \pm 1.09 \pm 0.02$	7.03 ± 1.42
$\pi^- \phi$	P'_C, P_{EW}	< 0.15	$0.28 \pm 0.004 \pm 0.055 \pm 0.003$	0.04 ± 0.02
$\pi^0 \rho^-$	T, C, P, P_A, P_{EW}	$\star 10.9 \pm 1.4$	$12.9 \pm 0.73 \pm 2.30 \pm 0.12$	12.15 ± 2.52
$\eta \rho^-$	$T, C, P, P_C, P_A, P_{EW}$	7.0 ± 2.9	$8.16 \pm 0.48 \pm 1.43 \pm 0.07$	5.26 ± 1.19
$\eta' \rho^-$	$T, C, P, P_C, P_A, P_{EW}$	$\star 9.7 \pm 2.2$	$6.0 \pm 0.34 \pm 0.97 \pm 0.05$	5.66 ± 1.25
$\pi^+ \rho^-$	$T, E, P, (P_E), P_A$	$\star 14.6 \pm 1.6$	$12.4 \pm 0.64 \pm 3.20 \pm 0.38$	15.20 ± 1.52
$\pi^- \rho^+$	$T, E, P, (P_E)$	$\star 8.4 \pm 1.1$	$6.04 \pm 0.47 \pm 1.70 \pm 0.25$	8.22 ± 1.06
$\pi^0 \rho^0$	$C, C', E, P, P_A, (P_E), P_{EW}$	$\star 2 \pm 0.5$	$1.32 \pm 0.47 \pm 0.09 \pm 0.14$	2.24 ± 0.93
$\pi^0 \omega$	$C, C', E, P, P_A, (P_E), P_{EW}$	< 0.5	$2.31 \pm 0.88 \pm 0.24 \pm 0.07$	1.02 ± 0.66
$\pi^0 \phi$	P'_C, P_{EW}	< 0.15	$0.13 \pm 0.002 \pm 0.025 \pm 0.001$	0.02 ± 0.01
$\eta \rho^0$	$C, C', E, P, P_C, P'_C, P_A, (P_E), P_{EW}$	< 1.5	$4.41 \pm 1.15 \pm 0.39 \pm 0.17$	0.54 ± 0.32
$\eta \omega$	$C, C', E, P, P_C, P'_C, P_A, (P_E), P_{EW}$	$0.94^{+0.40}_{-0.31}$	$0.89 \pm 0.30 \pm 0.08 \pm 0.09$	1.12 ± 0.44
$\eta \phi$	P'_C, P_{EW}	< 0.5	$0.077 \pm 0.001 \pm 0.015 \pm 0.0008$	0.01 ± 0.01
$\eta' \rho^0$	$C, C', E, P, P_C, P'_C, (P_E), P_{EW}$	< 1.3	$3.19 \pm 0.77 \pm 0.29 \pm 0.12$	0.63 ± 0.33
$\eta' \omega$	$C, C', E, P, P_C, P'_C, (P_E), P_{EW}$	$1.0^{+0.5}_{-0.4}$	$0.95 \pm 0.21 \pm 0.05 \pm 0.06$	1.24 ± 0.47
$\eta' \phi$	P'_C, P_{EW}	< 0.5	$0.05 \pm 0.0008 \pm 0.01 \pm 0.0005$	0.01 ± 0.01
$K^- K^{*0}$	P, P_A	< 1.1	$0.59 \pm 0.06 \pm 0.10 \pm 0.01$	0.46 ± 0.03
$K^0 K^{*-}$	P		$0.44 \pm 0.03 \pm 0.09 \pm 0.004$	0.31 ± 0.03
$K^0 \bar{K}^{*0}$	P		$0.41 \pm 0.02 \pm 0.08 \pm 0.004$	0.29 ± 0.03
$\bar{K}^0 K^{*0}$	P, P_A		$0.55 \pm 0.05 \pm 0.09 \pm 0.01$	0.43 ± 0.02
$\pi^- \bar{K}^{*0}$	P, P_A	$\star 10.1 \pm 0.9$	$10.0 \pm 0.95 \pm 1.78 \pm 0.15$	10.47 ± 0.60
$\pi^0 K^{*-}$	T, C, P, P_A, P_{EW}	$\star 8.2 \pm 1.9$	$6.23 \pm 0.51 \pm 0.98 \pm 0.07$	9.79 ± 2.95
ηK^{*-}	$T, C, P, P_C, P_A, P_{EW}$	$\star 19.3 \pm 1.6$	$17.3 \pm 0.8 \pm 2.4 \pm 0.3$	16.57 ± 2.58
$\eta' K^{*-}$	$T, C, P, P_C, P_A, P_{EW}$	$4.8^{+1.8}_{-1.6}$	$3.31 \pm 0.44 \pm 0.38 \pm 0.13$	3.43 ± 1.43
$K^- \rho^0$	T, C', P, P_{EW}	$\star 3.7 \pm 0.5$	$3.97 \pm 0.25 \pm 0.80 \pm 0.04$	3.97 ± 0.90
$K^- \omega$	T, C', P, P'_C, P_{EW}	$\star 6.5 \pm 0.4$	$6.52 \pm 0.73 \pm 1.13 \pm 0.06$	6.43 ± 1.49
$K^- \phi$	P, P'_C, P_A, P_{EW}	$\star 8.8 \pm 0.7$	$8.38 \pm 1.21 \pm 0.69 \pm 0.50$	8.34 ± 1.31
$\bar{K}^0 \rho^-$	P	$\star 8 \pm 1.5$	$7.74 \pm 0.47 \pm 1.55 \pm 0.07$	7.09 ± 0.77
$\pi^+ K^{*-}$	T, P, P_A	$\star 8.4 \pm 0.8$	$8.40 \pm 0.77 \pm 1.46 \pm 0.14$	8.35 ± 0.50
$\pi^0 \bar{K}^{*0}$	C, P, P_A, P_{EW}	$\star 3.3 \pm 0.6$	$3.35 \pm 0.36 \pm 0.65 \pm 0.08$	3.89 ± 1.98
$\eta \bar{K}^{*0}$	C, P, P_C, P_A, P_{EW}	$\star 15.9 \pm 1$	$16.6 \pm 0.7 \pm 2.3 \pm 0.3$	16.34 ± 2.48
$\eta' \bar{K}^{*0}$	$C, P, P_C, P'_C, P_A, P_{EW}$	$\star 2.8 \pm 0.6$	$3.0 \pm 0.5 \pm 0.3 \pm 0.1$	3.14 ± 1.24
$K^- \rho^+$	T, P	$\star 7 \pm 0.9$	$8.27 \pm 0.44 \pm 1.65 \pm 0.07$	8.28 ± 0.80
$\bar{K}^0 \rho^0$	C', P, P_{EW}	$\star 4.7 \pm 0.4$	$4.59 \pm 0.34 \pm 0.79 \pm 0.04$	4.97 ± 1.14
$\bar{K}^0 \omega$	C', P, P'_C, P_{EW}	$\star 4.8 \pm 0.6$	$4.80 \pm 0.61 \pm 0.95 \pm 0.05$	4.82 ± 1.26
$\bar{K}^0 \phi$	P, P'_C, P_A, P_{EW}	$\star 7.3 \pm 0.7$	$7.77 \pm 1.12 \pm 0.64 \pm 0.46$	7.72 ± 1.21

[14], where the ratio even reached 0.97 in Scheme C.

The $B^- \rightarrow K^- K^0$, $B^0 \rightarrow K^0 \bar{K}^0$ decays are purely penguin decays. From Table III one can see that their branching fractions given in our FAT approach are in much better agreement with experimental data than the previous conventional flavor diagram approach [14]. The penguin amplitude is mostly determined by the more precise measurements of $B^0 \rightarrow \pi K$ decays. There is only SU(3) breaking effect between KK final states and πK final states. Our results for KK final states are larger, because we considered SU(3) breaking effect and the previous conventional flavor diagram approach not. For the $B \rightarrow PV$ decays, where a vector meson is emitted from the weak interaction point, such as $B^- \rightarrow K^- K^{*0}$, $\bar{B}^0 \rightarrow K^{*0} \bar{K}^0$ decay modes, there is an extra penguin annihilation diagram P_A , in addition to the penguin emission diagram P . We find that the theoretical prediction for $B(B^- \rightarrow K^- K^{*0})$ is a little larger than $B(B^- \rightarrow K^{*-} K^0)$, and $B(\bar{B}^0 \rightarrow \bar{K}^{*0} K^0)$ is a little larger than $B(\bar{B}^0 \rightarrow \bar{K}^{*0} K^0)$. All these results are larger than the previous conventional flavor diagram approach [14], but in agreement with the prediction from SCET [19].

We did not show the decay $\bar{B}^0 \rightarrow K^+ K^-$ in our table. This decay is measured with $B(\bar{B}^0 \rightarrow K^+ K^-) = 0.13 \pm 0.05$ that is less than 3σ significance, therefore, we did not include this measurement into our χ^2 fit program. Theoretically, this decay is dominated by the exchange diagram E and penguin exchange diagram P_E . Since not enough experimental data to fit the P_E contribution, our result for this channel is only from the W-exchange diagram χ^E fitted from $B^0 \rightarrow \pi^0 \pi^0(\rho^0)$, $\pi^+ \pi^-$ decay modes. With only one contribution, our result $B(\bar{B}^0 \rightarrow K^+ K^-) = 1.30 \pm 0.25 \pm 0.00 \pm 0.13$ is one order magnitude higher than the central value of experimental data. This should be resolved with more precise experimental data to fit the P_E contribution in the future.

The $B \rightarrow PP$ decays with flavour singlet mesons $\eta^{(\prime)}$ in the final states are more complicated than other decay channels. There are complicated $\eta - \eta'$ mixing effect and most of them include almost all kinds of topologies except for E diagram. As shown in Eq.(31), $|P_C|/|P|$ is close to $|C|/|T|$ in ηK decays. The flavor-singlet QCD penguin diagram P_C in FAT approach and also in the conventional topological diagram approach [14] play the same role as the long-distance charming penguin $A_{ccg}^{PP}, A_{ccg}^{VP}$ in SCET [19]. It has an important effect on the large branching fraction of $B \rightarrow K\eta'$ and other observations of this type of penguin dominant decays. In the conventional topological diagram approach, the $\eta - \eta'$ mixing angle ϕ is a free parameter to be fitted from hadronic B decay data as $\phi = 46^\circ$ for

$B \rightarrow PP$ and $\phi = 43^\circ$ for $B \rightarrow PV$ decays [14]. However, the fitting is not so successful as expected with the branching fraction of $B^- \rightarrow \pi^- \eta'$ two times larger than the experimental value. These decays are recently reanalyzed with better results for $B \rightarrow PP$ decays in ref.[12]. It is noted that we fix the mixing angles from other experiments for the $\eta - \eta'$, resulting in better results for these decays.

TABLE V: Branching fractions ($\times 10^{-6}$) of various $\bar{B}_s \rightarrow PP$ and $\bar{B}_s \rightarrow PV$ decays. We also show the experimental data [21] and results from conventional flavor diagram approach [14] for comparison.

Mode	Amplitudes	Exp	This work	Flavor diagram
$\pi^- K^+$	T, P	5.5 ± 0.6	$6.98 \pm 0.02 \pm 1.40 \pm 0.02$	5.86 ± 0.78
$\pi^0 \eta$	$C, E, P_C, (P_E), P_{EW}$	< 1000	$0.10 \pm 0.013 \pm 0.013 \pm 0.003$	0.12 ± 0.07
$\pi^0 \eta'$	$C, E, P_C, (P_E), P_{EW}$		$0.11 \pm 0.01 \pm 0.02 \pm 0.002$	0.12 ± 0.06
$\pi^0 K^0$	C, P, P_{EW}		$0.97 \pm 0.16 \pm 0.2 \pm 0.003$	2.25 ± 0.33
$\eta \eta$	$C, E, P, P_C, (P_E), P_{EW}$	< 1500	$11.4 \pm 0.42 \pm 2.25 \pm 0.04$	8.24 ± 1.53
$\eta \eta'$	$C, E, P, P_C, (P_E), P_{EW}$		$40.4 \pm 2.06 \pm 8.14 \pm 0.13$	33.47 ± 3.64
ηK^0	C, P, P_C, P_{EW}		$0.55 \pm 0.11 \pm 0.08 \pm 0.002$	0.97 ± 0.16
$\eta' \eta'$	$C, E, P, P_C, (P_E), P_{EW}$		$42.1 \pm 3.48 \pm 8.38 \pm 0.13$	41.48 ± 6.25
$\eta' K^0$	C, P, P_C, P_{EW}		$2.15 \pm 0.15 \pm 0.30 \pm 0.01$	3.94 ± 0.39
$K^+ K^-$	$T, E, P, (P_E)$	24.9 ± 1.7	$16.7 \pm 0.46 \pm 3.27 \pm 0.16$	17.90 ± 2.98
$K^0 \bar{K}^0$	P	< 66	$17.5 \pm 0.47 \pm 3.50 \pm 0.16$	17.48 ± 2.36
$\pi^- K^{*+}$	T, P		$11.1 \pm 0.02 \pm 2.21 \pm 0.03$	7.92 ± 1.02
$\pi^0 \phi$	C, P_{EW}		$0.26 \pm 0.02 \pm 0.05 \pm 0.001$	1.94 ± 1.14
$\pi^0 K^{*0}$	C, P, P_{EW}		$1.22 \pm 0.25 \pm 0.24 \pm 0$	3.07 ± 1.20
$\eta \rho^0$	$C', E, P'_C, (P_E), P_{EW}$		$0.13 \pm 0.02 \pm 0.02 \pm 0.003$	0.34 ± 0.21
$\eta \omega$	$C', E, P'_C, (P_E), P_{EW}$		$3.25 \pm 0.10 \pm 0.63 \pm 0.03$	0.15 ± 0.16
$\eta \phi$	$C, P, P_C, P'_C, P_{EW}, P_A$		$0.80 \pm 0.22 \pm 0.53 \pm 0.14$	0.39 ± 0.39
ηK^{*0}	C, P, P_C, P_{EW}, P_A		$0.99 \pm 0.18 \pm 0.16 \pm 0.01$	1.44 ± 0.54
$\eta' \rho^0$	$C', E, P'_C, (P_E), P_{EW}$		$0.37 \pm 0.07 \pm 0.05 \pm 0.01$	0.31 ± 0.19
$\eta' \omega$	$C', E, P'_C, (P_E), P_{EW}$		$3.97 \pm 0.15 \pm 0.79 \pm 0.04$	0.14 ± 0.14
$\eta' \phi$	$C, P, P_C, P'_C, P_{EW}, P_A$		$13.0 \pm 1.05 \pm 0.98 \pm 0.67$	5.48 ± 1.84
$\eta' K^{*0}$	C, P, P_C, P_{EW}, P_A		$1.64 \pm 0.15 \pm 0.22 \pm 0.03$	1.65 ± 0.60
$K^+ \rho^-$	T, P, P_A		$17.5 \pm 0 \pm 3.5 \pm 0.2$	14.63 ± 1.46
$K^+ K^{*-}$	$T, E, P, P_A, (P_E)$		$8.85 \pm 1.06 \pm 1.04 \pm 0.37$	8.03 ± 0.48
$K^- K^{*+}$	$T, E, P, (P_E)$		$6.39 \pm 0.38 \pm 1.35 \pm 0.07$	7.98 ± 0.77
$K^0 \rho^0$	C', P, P'_C, P_A, P_{EW}		$1.61 \pm 1.10 \pm 0.31 \pm 0.02$	0.56 ± 0.24
$K^0 \omega$	C', P, P'_C, P_A, P_{EW}		$1.43 \pm 0.88 \pm 0.25 \pm 0.02$	0.58 ± 0.25
$K^0 \phi$	P, P'_C, P_{EW}		$0.35 \pm 0.04 \pm 0.06 \pm 0.003$	0.41 ± 0.07
$K^0 \bar{K}^{*0}$	P, P_A		$9.28 \pm 1.14 \pm 1.21 \pm 0.34$	9.33 ± 0.54
$\bar{K}^0 K^{*0}$	P		$6.31 \pm 0.38 \pm 1.26 \pm 0.06$	6.32 ± 0.68

For the sub-leading contribution electroweak penguin diagram P_{EW} , four free parameters (two magnitudes and two phases) are introduced to be fitted from experiments [14] with non-negligible strong phase for $B \rightarrow PP$ decays and even considerable magnitude for $B \rightarrow VP$ decays. As stated in the last section, we did not include any free parameters for this kind of diagrams but use factorization formulas to make predictions. For the $B \rightarrow \pi(\rho)K(K^*)$ decays, their branching fractions are in good agreement with data by the non-negligible factorization P_{EW} diagram contribution. For example, the central value of $B(B^- \rightarrow \pi^0 K^-)$ is equal to data precisely attributed to the non-negligible correction effect from P_{EW} diagram.

Most of the $B_s \rightarrow PP, PV$ decays are not well measured in the experiments. Therefore, we do not include any of the B_s data in our χ^2 fit program. Their branching ratios are all as predictions in our FAT approach shown in Table V. The accuracy of these predictions rely on the assumption that the mechanism for B and B_s decays are the same. If there are enough data for B_s decays, one need do the χ^2 fit again. In this table, we do not include the channel $B_s \rightarrow \pi^+\pi^-$. Our result (with only W-exchange contribution) for this channel $B(\bar{B}_s \rightarrow \pi^+\pi^-) = 0.051 \pm 0.001 \pm 0 \pm 0.005$ is much smaller than the experimental data measured by LHCb and CDF shown in Eq.(8). As stated in the last section, this decay is dominated by the penguin exchange diagram P_E [80], which can only be fitted from this mode $B_s \rightarrow \pi^+\pi^-$. One measurement to determine one parameter is not a perfect way of χ^2 fitting. Therefore we look forward to more data to determine this contribution in other modes and to test our FAT in the future. Similarly, without this contribution, we are unable to predict a number of decay channels, dominated by this contribution: $B^0 \rightarrow K^+K^-$, $B^0 \rightarrow K^{*+}K^-$, $B^0 \rightarrow K^+K^{*-}$, $B_s \rightarrow \pi^+\rho^-$, $B_s \rightarrow \pi^-\rho^+$, $B_s \rightarrow \pi^0\rho^0$, $B_s \rightarrow \pi^0\omega$ and $B_s \rightarrow \pi^0\pi^0$.

D. CP asymmetry study

The charmless B decays are important mostly because of its large direct CP asymmetry in B decays. Due to the CKM matrix elements suppression of tree diagram, the penguin diagram contribution is at the same order magnitude as the tree diagram. The large CKM phase difference between these two kinds of diagram almost guarantees the existence of large direct CP asymmetry. That is not the whole story. The direct CP asymmetry parameter is also proportional to the strong phase difference between these two diagrams. Unfortunately, the strong phase is mostly from non-perturbative QCD dynamics. That is the reason why

TABLE VI: The direct CP asymmetries (\mathcal{A}) and mixing-induced CP asymmetries (\mathcal{S}) of $\bar{B} \rightarrow PP$ decays. We also show the results from conventional flavor diagram approach [14] for comparison.

Mode	\mathcal{A}_{exp}	$\mathcal{A}_{\text{this work}}$	$\mathcal{A}_{\text{Flavor diagram}}$	\mathcal{S}_{exp}	$\mathcal{S}_{\text{this work}}$	$\mathcal{S}_{\text{Flavor diagram}}$
$\pi^+\pi^-$	$\star 0.31 \pm 0.05$	0.31 ± 0.04	0.326 ± 0.081	$\star -0.67 \pm 0.06$	-0.60 ± 0.03	-0.717 ± 0.061
$\pi^0\pi^0$	0.43 ± 0.24	0.57 ± 0.06	0.611 ± 0.113		0.58 ± 0.06	0.454 ± 0.112
$\pi^0\eta$		-0.16 ± 0.16	0.566 ± 0.114		-0.98 ± 0.04	-0.098 ± 0.338
$\pi^0\eta'$		0.39 ± 0.14	0.385 ± 0.114		-0.90 ± 0.07	0.142 ± 0.234
$\eta\eta$		-0.85 ± 0.06	-0.405 ± 0.129		0.33 ± 0.12	-0.796 ± 0.077
$\eta\eta'$		-0.97 ± 0.04	-0.394 ± 0.117		-0.20 ± 0.15	-0.903 ± 0.049
$\eta'\eta'$		-0.87 ± 0.07	-0.122 ± 0.136		-0.46 ± 0.14	-0.964 ± 0.037
$\pi^0 K_s$	0.00 ± 0.13	-0.14 ± 0.03	-0.173 ± 0.019	$\star 0.58 \pm 0.17$	0.73 ± 0.01	0.754 ± 0.014
ηK_s		-0.30 ± 0.10	-0.301 ± 0.041		0.68 ± 0.04	0.592 ± 0.035
$\eta' K_s$	0.06 ± 0.04	0.030 ± 0.004	0.022 ± 0.006	$\star 0.63 \pm 0.06$	0.69 ± 0.00	0.685 ± 0.004
$K^0\bar{K}^0$		-0.057 ± 0.002	0.017 ± 0.041	0.8 ± 0.5	0.099 ± 0.002	0
$\pi^-\pi^0$	0.03 ± 0.04	-0.026 ± 0.003	0.069 ± 0.027			
$\pi^-\eta$	-0.14 ± 0.07	-0.14 ± 0.07	-0.081 ± 0.074			
$\pi^-\eta'$	0.06 ± 0.16	0.37 ± 0.07	0.374 ± 0.087			
$\pi^- K^0$	-0.017 ± 0.016	0.0027 ± 0.0001	0			
$\pi^0 K^-$	0.037 ± 0.021	0.065 ± 0.024	0.047 ± 0.025			
ηK^-	$\star -0.37 \pm 0.08$	-0.22 ± 0.08	-0.426 ± 0.043			
$\eta' K^-$	0.013 ± 0.017	-0.021 ± 0.007	-0.027 ± 0.008			
$K^- K^0$	-0.21 ± 0.14	-0.057 ± 0.002	0			
$\pi^+ K^-$	$\star -0.082 \pm 0.006$	-0.081 ± 0.005	-0.080 ± 0.011			

the QCD factorization and soft-collinear effective theory can predict the branching ratios of the charmless B decays well but make wrong prediction or no prediction for the direct CP asymmetries. There are already 3 good measurements of direct CP asymmetry measurements in $B \rightarrow PP$ decays and 3 in $B \rightarrow PV$ decays indicated as a star in Tables VI and VII. There are also 5 mixing induced CP asymmetry measurements for the neutral B meson decays to be used in our χ^2 program. We give the direct CP and mixing-induced CP asymmetries of corresponding B decay modes in Tables VI and VII. From the CP asymmetry formula in eq.(13), we know that the CP asymmetry is proportional to the difference of B meson and \bar{B} meson. Thus the theoretical uncertainty from hadronic parameters mostly cancel, because they contribute to the charge conjugate modes equally. The main theoretical uncertainty for CP asymmetry parameters is from the experimental data and CKM angle. We did not show the individual uncertainty, but the combined one in these CP asymmetry tables.

TABLE VII: The direct CP asymmetries (\mathcal{A}) and mixing-induced CP asymmetries (\mathcal{S}) of $\bar{B} \rightarrow PV$ decays. We also show the results from conventional flavor diagram approach [14] for comparison.

Mode	\mathcal{A}_{exp}	$\mathcal{A}_{\text{this work}}$	$\mathcal{A}_{\text{Flavor diagram}}$	\mathcal{S}_{exp}	$\mathcal{S}_{\text{this work}}$	$\mathcal{S}_{\text{Flavor diagram}}$
$\pi^+ \rho^-$	0.13 ± 0.06	0.15 ± 0.03	0.120 ± 0.027	0.07 ± 0.14	0.011 ± 0.034	-0.049 ± 0.074
$\pi^- \rho^+$	-0.08 ± 0.08	-0.44 ± 0.03	-0.136 ± 0.053	0.05 ± 0.08	-0.093 ± 0.040	-0.024 ± 0.065
$\pi^0 \rho^0$	-0.27 ± 0.24	0.36 ± 0.08	-0.043 ± 0.121	-0.23 ± 0.34	0.19 ± 0.16	-0.229 ± 0.112
$\pi^0 \omega$		-0.024 ± 0.068	-0.188 ± 0.185		0.29 ± 0.05	-0.315 ± 0.195
$\eta \rho^0$		-0.23 ± 0.03	-0.264 ± 0.215		-0.023 ± 0.038	-0.628 ± 0.196
$\eta \omega$		-0.30 ± 0.13	0.054 ± 0.137		0.43 ± 0.09	-0.461 ± 0.113
$\eta' \rho^0$		0.088 ± 0.085	-0.440 ± 0.317		-0.48 ± 0.07	-0.714 ± 0.252
$\eta' \omega$		-0.85 ± 0.17	-0.005 ± 0.259		0.50 ± 0.26	-0.624 ± 0.120
$K_s \rho^0$	0.04 ± 0.20	-0.085 ± 0.059	0.069 ± 0.053	0.5 ± 0.21	0.88 ± 0.05	0.643 ± 0.036
$K_s \omega$	0 ± 0.4	0.25 ± 0.10	-0.053 ± 0.055	$\star 0.7 \pm 0.21$	0.70 ± 0.04	0.789 ± 0.028
$K_s \phi$	-0.01 ± 0.14	-0.006 ± 0.001	0	$\star 0.59 \pm 0.14$	0.70 ± 0.00	0.718 ± 0.000
$\bar{K}^0 K^{*0}$		-0.10 ± 0.02	0		-0.90 ± 0.03	0
$K^0 \bar{K}^{*0}$		-0.18 ± 0.01	0		0.89 ± 0.03	0
$\pi^- \rho^0$	$0.18^{+0.09}_{-0.17}$	-0.45 ± 0.04	-0.239 ± 0.084			
$\pi^- \omega$	-0.04 ± 0.06	0.054 ± 0.052	0.075 ± 0.067			
$\pi^0 \rho^-$	0.02 ± 0.11	0.16 ± 0.02	0.053 ± 0.094			
$\eta \rho^-$	0.11 ± 0.11	-0.11 ± 0.02	0.162 ± 0.072			
$\eta' \rho^-$	0.26 ± 0.17	0.45 ± 0.05	0.223 ± 0.137			
$\pi^- K^{*0}$	-0.04 ± 0.09	0.005 ± 0.001	0			
$\pi^0 K^{*-}$	-0.06 ± 0.24	0.088 ± 0.040	-0.116 ± 0.092			
ηK^{*-}	0.02 ± 0.06	-0.17 ± 0.02	-0.016 ± 0.037			
$\eta' K^{*-}$	-0.26 ± 0.27	-0.45 ± 0.09	-0.391 ± 0.162			
$K^- \rho^0$	$\star 0.37 \pm 0.10$	0.59 ± 0.06	0.306 ± 0.100			
$K^- \omega$	0.02 ± 0.05	0.19 ± 0.09	0.010 ± 0.080			
$K^- \phi$	0.04 ± 0.04	-0.006 ± 0.001	0			
$K^- K^{*0}$		-0.10 ± 0.02	0			
$K^0 K^{*-}$		-0.18 ± 0.01	0			
$\bar{K}^0 \rho^-$	-0.12 ± 0.17	0.009 ± 0.000	0			
$\pi^+ K^{*-}$	$\star -0.22 \pm 0.06$	-0.20 ± 0.04	-0.217 ± 0.048			
$\pi^0 \bar{K}^{*0}$	-0.15 ± 0.13	-0.27 ± 0.05	-0.332 ± 0.114			
$\eta \bar{K}^{*0}$	$\star 0.19 \pm 0.05$	0.065 ± 0.011	0.099 ± 0.028			
$\eta' \bar{K}^{*0}$	-0.07 ± 0.18	0.059 ± 0.049	0.069 ± 0.152			
$K^- \rho^+$	0.21 ± 0.11	0.59 ± 0.01	0.134 ± 0.053			

Since the CKM matrix elements are enhanced for penguin diagram compared with the tree diagrams in the $B \rightarrow \pi(\rho)K^{(*)}$ decays by $b \rightarrow s$ transition, there is large interference effect between these two kinds of Feynman diagrams, which results in larger CP asymmetry in these decays. $A_{CP}(\bar{B}^0 \rightarrow \pi^+ K^-)$ is the first measurement of direct CP asymmetry in

B decays. From table III, one can see that $B^- \rightarrow \pi^0 K^-$ decay has the same dominant decay amplitude T and P as $\bar{B}^0 \rightarrow \pi^+ K^-$ decay, thus one expects the same direct CP asymmetry [8]. However, experimentally these two direct CP asymmetry is quite different, even with an opposite sign. That is the so-called πK CP-puzzle. In our study, the sub-leading contribution C and P_{EW} are not negligible, especially C with a large strong phase, therefore this puzzle is resolved.

There is one category of decays with pure penguin contributions, such as $B^- \rightarrow K^- K^0$, $\bar{B}^0 \rightarrow K^0 \bar{K}^0$, $B^- \rightarrow \pi^- \bar{K}^0$, $B^- \rightarrow \pi^- \bar{K}^{*0}$, $B^- \rightarrow \rho^- \bar{K}^0$ and $\bar{B}_s \rightarrow K^0 \bar{K}^0$. Their direct CP asymmetry is expected to be zero, at leading order approximation. The very small (not zero) CP asymmetry is from the small up quark or charm quark penguin contribution interference with the dominant top quark contribution. Any large CP asymmetry measurement for these decays will be a clear signal of new physics. In Table VI, we did not show the decay channel $\bar{B}^0 \rightarrow K^+ K^-$. The reason is that there should be two major contributions for this channel, but we calculate only one (tree level W exchange digram). The other contribution from penguin-exchange (P_E) diagram is not fitted because of lack of experimental data. The branching ratio of this channel with only one contribution, discussed in previous subsection, is far from the central value of experimental data. This may indicate the importance of the penguin-exchange (P_E) diagram, which will give a large direct CP asymmetry for this channel. Similarly, we can not predict the CP asymmetry for $B^0 \rightarrow K^{*+} K^-$ and $B^0 \rightarrow K^+ K^{*-}$.

The mixing induced CP asymmetries in neutral B decays into final CP eigenstates are dominated by the $B^0 - \bar{B}^0$ mixing phase with little dependence on strong phases. That is the reason why it is usually used for searching possible new physics. For example, the measured mixing induced CP asymmetry parameters of $S_{CP}(\pi^+ \pi^-)$, $S_{CP}(\pi^0 K_S)$, $S_{CP}(\eta' K_S)$ and $S_{CP}(\phi K_S)$ have received much attention in experiment and in theoretical aspect due to little theoretical uncertainty. Currently, there is a good agreement between theoretical calculations and experimental data shown in Table VI and VII. Further study is needed from both theoretical and experimental effort in the future.

There are only two channels of B_s decays, namely $B_s \rightarrow K^+ K^-$ and $\bar{B}_s \rightarrow K^+ \pi^-$ with CP asymmetry measurements shown in table VIII. As stated, we do not include any B_s data in our χ^2 fit. All the B_s results are predictions. It is easy to see that our predictions for these two channels agree with data within error-bar. There is no CP asymmetry measurement for

TABLE VIII: The direct CP asymmetries (\mathcal{A}) and mixing-induced CP asymmetries (\mathcal{S}) of $\bar{B}_s \rightarrow PP$ decays. We also show the results from conventional flavor diagram approach [14] for comparison.

Mode	\mathcal{A}_{exp}	$\mathcal{A}_{\text{this work}}$	$\mathcal{A}_{\text{Flavor diagram}}$	\mathcal{S}_{exp}	$\mathcal{S}_{\text{this work}}$	$\mathcal{S}_{\text{Flavor diagram}}$
$\pi^0 \eta$		0.90 ± 0.05	-0.165 ± 0.292		0.19 ± 0.11	0.836 ± 0.198
$\pi^0 \eta'$		0.44 ± 0.10	0.259 ± 0.335		-0.79 ± 0.07	0.953 ± 0.116
$\pi^0 K_s$		0.87 ± 0.05	0.724 ± 0.054		0.0096 ± 0.0905	0.302 ± 0.080
$\eta \eta$		-0.11 ± 0.01	-0.116 ± 0.018		-0.14 ± 0.01	-0.095 ± 0.020
$\eta \eta'$		-0.013 ± 0.005	-0.009 ± 0.003		-0.038 ± 0.006	-0.036 ± 0.007
ηK_s		0.74 ± 0.17	0.452 ± 0.057		0.31 ± 0.16	0.787 ± 0.042
$\eta' \eta'$		0.042 ± 0.006	0.016 ± 0.009		-0.055 ± 0.006	0.028 ± 0.009
$\eta' K_s$		-0.58 ± 0.06	-0.367 ± 0.089		-0.029 ± 0.099	0.191 ± 0.090
$K^+ K^-$	-0.14 ± 0.11	-0.11 ± 0.02	-0.090 ± 0.021	0.30 ± 0.13	0.097 ± 0.022	0.140 ± 0.030
$K^0 \bar{K}^0$		0.0027 ± 0.0001	-0.075 ± 0.035		0.069 ± 0.000	-0.039 ± 0.001
$\pi^- K^+$	0.28 ± 0.04	0.16 ± 0.01	0.266 ± 0.033			

$B_s \rightarrow PV$ decays. Our theoretical predictions are shown in table IX, together with results from the conventional flavor diagram approach. It is noted that there is large differences between predictions of these two approaches for example: $B_s \rightarrow \pi^0 \phi$, $B_s \rightarrow \eta \rho^0$, $B_s \rightarrow \eta' \rho^0$ and $B_s \rightarrow \eta' \omega$ etc. Many of these entries with large CP asymmetry predicted, can be tested by the experiments in the near future. Similar to the situation of branching ratios, we also did not give predictions for the CP asymmetry of decays $B_s \rightarrow \pi^+ \pi^-$, $B_s \rightarrow \pi^+ \rho^-$, $B_s \rightarrow \pi^- \rho^+$, $B_s \rightarrow \pi^0 \rho^0$, $B_s \rightarrow \pi^0 \omega$ and $B_s \rightarrow \pi^0 \pi^0$, lack of the information of penguin exchange diagram (P_E).

E. The flavor $SU(3)$ asymmetry

The flavor $SU(3)$ symmetry is broken by the difference in the u, d and s quark masses, especially the difference in d and s quark masses. The $SU(3)$ breaking is also very important in explaining the different size of CP asymmetry in different charmless $B \rightarrow PP$, PV decays. We consider the flavor $SU(3)$ violating contributions assisted by factorization hypothesis where the source of $SU(3)$ asymmetries are mainly from decay constants and weak transition form factors. It is not necessary to include different $SU(3)$ asymmetry phases for different modes, because our numerical results of branching ratios and CP asymmetry parameters

TABLE IX: The direct CP asymmetries (\mathcal{A}) and mixing-induced CP asymmetries (\mathcal{S}) of $\bar{B}_s \rightarrow PV$ decays. We also show the results from conventional flavor diagram approach [14] for comparison.

Mode	$\mathcal{A}_{this\ work}$	$\mathcal{A}_{Flavor\ diagram}$	$\mathcal{S}_{this\ work}$	$\mathcal{S}_{Flavor\ diagram}$
$\pi^0\phi$	0.89 ± 0.04	0.073 ± 0.201	-0.25 ± 0.07	0.439 ± 0.171
$\eta\rho^0$	-0.46 ± 0.38	0.323 ± 0.136	0.88 ± 0.19	-0.002 ± 0.168
$\eta\omega$	-0.086 ± 0.071	-0.432 ± 0.271	-0.31 ± 0.06	-0.238 ± 0.296
$\eta\phi$	0.083 ± 0.113	0.428 ± 0.504	0.39 ± 0.15	0.534 ± 0.400
$\eta'\rho^0$	-0.67 ± 0.10	0.323 ± 0.136	-0.72 ± 0.07	-0.002 ± 0.168
$\eta'\omega$	0.33 ± 0.06	-0.432 ± 0.271	-0.14 ± 0.07	-0.238 ± 0.296
$\eta'\phi$	-0.010 ± 0.017	0.043 ± 0.090	0.047 ± 0.015	0.166 ± 0.057
K^+K^{*-}	-0.30 ± 0.04	-0.217 ± 0.048	-0.78 ± 0.06	0
K^-K^{*+}	0.39 ± 0.04	0.134 ± 0.053	0.67 ± 0.05	0
$K_s\rho^0$	-0.42 ± 0.15	-0.124 ± 0.453	0.78 ± 0.08	-0.348 ± 0.285
$K_s\omega$	-0.010 ± 0.151	-0.029 ± 0.436	-0.32 ± 0.30	0.928 ± 0.110
$K_s\phi$	-0.003 ± 0.033	0	-0.85 ± 0.01	-0.692 ± 0.000
$K^0\bar{K}^{*0}$	0.002 ± 0.001	0	-0.74 ± 0.05	0
\bar{K}^0K^{*0}	0.009 ± 0.000	0	0.83 ± 0.04	0
π^-K^{*+}	-0.30 ± 0.01	-0.136 ± 0.053		
π^0K^{*0}	-0.30 ± 0.06	-0.423 ± 0.158		
ηK^{*0}	0.57 ± 0.12	0.828 ± 0.123		
$\eta' K^{*0}$	-0.46 ± 0.10	-0.408 ± 0.273		
$K^+\rho^-$	0.16 ± 0.03	0.120 ± 0.027		

are in good agreement with experimental data shown in previous subsections.

As every decay mode include various topological diagrams, the precise flavor $SU(3)$ breaking effect, can not be separated from one another in $B \rightarrow PP, PV$ decays, are hard to be tested by experimental data. We show the flavor $SU(3)$ breaking effect in every topology

amplitude between $B \rightarrow \pi\pi$ and $B \rightarrow \pi K$, $B \rightarrow \eta\pi$ and $B \rightarrow \eta K$, as following:

$$\left| \frac{T(B^- \rightarrow \pi^0 K^-)}{V_{ub}V_{us}^*} \right| : \left| \frac{T(B^- \rightarrow \pi^0 \pi^-)}{V_{ub}V_{ud}^*} \right| = 1 : 0.83, \quad (34)$$

$$\left| \frac{C(B^- \rightarrow \pi^0 K^-)}{V_{ub}V_{us}^*} \right| : \left| \frac{C(B^- \rightarrow \pi^0 \pi^-)}{V_{ub}V_{ud}^*} \right| = 1 : 0.91, \quad (35)$$

$$\left| \frac{P(\bar{B}^0 \rightarrow \pi^+ K^-)}{V_{tb}V_{ts}^*} \right| : \left| \frac{P(\bar{B}^0 \rightarrow \pi^+ \pi^-)}{V_{tb}V_{td}^*} \right| = 1 : 0.89, \quad (36)$$

$$\left| \frac{P_C(B^- \rightarrow \eta K^-)}{V_{tb}V_{ts}^*} \right| : \left| \frac{P_C(B^- \rightarrow \eta \pi^-)}{V_{tb}V_{td}^*} \right| = 1 : 0.91. \quad (37)$$

From the above results, we find that the flavor $SU(3)$ breaking effects are around 10% because of different decay constants between f_π and f_K , or form factors $F^{B \rightarrow \pi}$ and $F^{B \rightarrow K}$. The flavor $SU(3)$ breaking effect in every topology amplitude between $B \rightarrow \pi\rho$ and $B \rightarrow \pi K^*$, $B \rightarrow \eta\rho$ and $B \rightarrow \eta K^*$ are also shown as following:

$$\left| \frac{T(B^- \rightarrow \pi^0 K^{*-})}{V_{ub}V_{us}^*} \right| : \left| \frac{T(B^- \rightarrow \pi^0 \rho^-)}{V_{ub}V_{ud}^*} \right| = 1 : 0.83, \quad (38)$$

$$\left| \frac{C(B^- \rightarrow K^{*-} \pi^0)}{V_{ub}V_{us}^*} \right| : \left| \frac{C(B^- \rightarrow \rho^- \pi^0)}{V_{ub}V_{ud}^*} \right| = 1 : 0.80, \quad (39)$$

$$\left| \frac{P(\bar{B}^0 \rightarrow \pi^+ K^{*-})}{V_{tb}V_{ts}^*} \right| : \left| \frac{P(\bar{B}^0 \rightarrow \pi^+ \rho^-)}{V_{tb}V_{td}^*} \right| = 1 : 0.74, \quad (40)$$

$$\left| \frac{P_C(B^- \rightarrow K^{*-} \eta)}{V_{tb}V_{ts}^*} \right| : \left| \frac{P_C(B^- \rightarrow \rho^- \eta)}{V_{tb}V_{td}^*} \right| = 1 : 0.80, \quad (41)$$

$$\left| \frac{P_A(\bar{B}^0 \rightarrow \pi^+ K^{*-})}{V_{tb}V_{ts}^*} \right| : \left| \frac{P_A(\bar{B}^0 \rightarrow \pi^+ \rho^-)}{V_{tb}V_{td}^*} \right| = 1 : 0.84. \quad (42)$$

It is easy to see that the flavor $SU(3)$ breaking effects are larger than 20% because of different decay constants between f_ρ and f_{K^*} , or different form factors between $A_0^{B \rightarrow \rho}$ and $A_0^{B \rightarrow K^*}$.

In previous flavor diagram approach, the charmless $B \rightarrow PP$ and $B \rightarrow PV$ decays are fitted separately with very different theoretical parameters. That implies large difference between pseudo-scalar meson and vector meson. To show this difference numerically, we have:

$$|T(B^- \rightarrow \pi^0 \pi^-)| : |T(B^- \rightarrow \pi^0 \rho^-)| = 1 : 1.64, \quad (43)$$

$$|C(B^- \rightarrow \pi^0 \pi^-)| : |C'(B^- \rightarrow \pi^- \rho^0)| = 1 : 1.43, \quad (44)$$

$$|P(\bar{B}^0 \rightarrow \pi^+ \pi^-)| : |P(\bar{B}^0 \rightarrow \pi^+ \rho^-)| = 1 : 0.66. \quad (45)$$

It is easy to see that this difference between π and ρ meson emission is indeed much larger than the so called flavor $SU(3)$ breaking effect between π and K meson, because the meson

decay constant $f_\rho > f_K$. The penguin amplitude (P) for the $\bar{B} \rightarrow \pi^+ \rho^-$ decay, even if with a larger decay constant, is smaller than the corresponding $\bar{B} \rightarrow \pi^+ \pi^-$ decay, because there is no chiral enhanced penguin contribution for a vector meson emission shown in eq.(6). If the emitted meson is a pseudo-scalar scalar meson in $B \rightarrow VP$ decays, its difference from $B \rightarrow PP$ decays is the $B \rightarrow V$ transition form factor from $B \rightarrow P$ transition form factor. For example, the following difference between two decay channels is $B \rightarrow \pi$ form factor and $B \rightarrow \rho$ form factor, which is smaller than the difference between π and ρ decay constant:

$$|T(B^- \rightarrow \pi^0 \pi^-)| : |T(B^- \rightarrow \rho^- \pi^0)| = 1 : 1.24, \quad (46)$$

$$|C(B^- \rightarrow \pi^0 \pi^-)| : |C(B^- \rightarrow \rho^- \pi^0)| = 1 : 1.25, \quad (47)$$

$$|P(\bar{B}^0 \rightarrow \pi^+ \pi^-)| : |P(\bar{B}^0 \rightarrow \rho^- \pi^+)| = 1 : 0.59, \quad (48)$$

$$|P_C(B^- \rightarrow \eta \pi^-)| : |P_C(B^- \rightarrow \rho^- \eta)| = 1 : 1.26. \quad (49)$$

The penguin amplitude (P) for the $\bar{B} \rightarrow \rho^- \pi^+$ decay, even if with a larger decay constant, is smaller than the corresponding $\bar{B} \rightarrow \pi^+ \pi^-$ decay, because the chiral enhanced penguin contribution cancel some of the factorization penguin contribution as a minus sign shown in eq.(6). For decays induced by $b \rightarrow s$ transition, we have:

$$|T(B^- \rightarrow \pi^0 K^-)| : |T(B^- \rightarrow \pi^0 K^{*-})| = 1 : 1.42, \quad (50)$$

$$|C(B^- \rightarrow \pi^0 K^-)| : |C(B^- \rightarrow K^{*-} \pi^0)| = 1 : 1.23, \quad (51)$$

$$|P(\bar{B}^0 \rightarrow \pi^+ K^-)| : |P(\bar{B}^0 \rightarrow \pi^+ K^{*-})| = 1 : 0.68, \quad (52)$$

$$|P_C(B^- \rightarrow \eta K^-)| : |P_C(B^- \rightarrow K^{*-} \eta)| = 1 : 1.24. \quad (53)$$

It is apparent that the difference characterized by the K and K^* decay constant is large.

IV. CONCLUSION

In this paper, we studied two-body charmless hadronic B decays in factorization assisted topological amplitude approach. Since factorization has been proven to all orders in α_s in the so called soft-collinear effective theory at leading order in Λ/m_b expansion, the color-favored tree emission diagram T was factorized into short-distance effective Wilson coefficients and decay constants and form factors, without free parameters. The flavor $SU(3)$ breaking effects are then automatically considered in different meson decay constants and transition form

factors. Factorization theorem is not proven in most other topological diagrams. They were considered as universal magnitudes (χ) and associated phases (ϕ) in the conventional flavor diagram approach to be fitted from experimental data. In our approach, the corresponding decay constants, form factors were factorized out from them before χ^2 fit assisted by factorization hypothesis to indicate the flavor $SU(3)$ breaking effect. In addition to the large tree and QCD-penguin diagrams studied in these types of decays, the electro-weak penguin contribution (P_{EW}) was also included, which is not negligible but essential for $B \rightarrow \pi K$ decays, especially for the CP asymmetry parameters. Unlike the previous conventional flavor diagram approach, this contribution was factorized into short-distance effective Wilson coefficients and decay constants and form factors, just like the color-favored tree emission diagram T .

There were 6 parameters $\chi^C(\phi^C)$, $\chi^{C'}(\phi^{C'})$ and $\chi^E(\phi^E)$ for tree diagrams C, E and 8 parameters $\chi^P(\phi^P)$, $\chi^{P_C}(\phi^{P_C})$, $\chi^{P'_C}(\phi^{P'_C})$ and $\chi^{P_A}(\phi^{P_A})$ for QCD-penguin diagrams to be fitted from 48 measured data of branching ratios and CP asymmetry parameters. Since $SU(3)$ breaking effects and the difference between pseudo-scalar and vector meson have been already considered in the decays constants and form factors, we can fit all the $B \rightarrow PP$, PV decays together. The number of free parameters is greatly reduced. These parameters were extracted precisely even for small parameters χ^E, ϕ^E , which had large uncertainties in conventional flavor diagram approach. Besides, the χ^2 per degree of freedom is smaller than the conventional flavor diagram approach, even with much more free parameters in their approach. With the fitted parameters, we predicted branching fractions of $B_{(s)} \rightarrow PP$, PV decay modes and their CP asymmetry parameters. The long-standing puzzles of $\pi\pi$ branching ratios and πK CP asymmetry have been resolved consistently with not too large color suppressed tree diagram contribution χ^C . For the B_s decays, we do not include any data as input in the χ^2 fit, but all as theoretical predictions, since very few channels have been poorly measured. The flavor $SU(3)$ breaking effect between π and K were approximately 10%, even more than 20% in ρ and K^* meson case and larger in π and ρ , K and K^* .

V. ACKNOWLEDGMENTS

We are grateful to Hsiang-nan Li, Wei Wang, Rui Zhou, Fusheng Yu, Ying Li and Qin Qin for useful discussion. We also thanks Fred James providing help for analyzing error bar

in Minuit program. The work is partly supported by National Science Foundation of China (11375208, 11521505, 11621131001 and 11235005).

-
- [1] A. J. Bevan *et al.* [BaBar and Belle Collaborations], *Eur. Phys. J. C* **74**, 3026 (2014) doi: 10.1140/epjc/s10052-014-3026-9 [arXiv:1406.6311 [hep-ex]].
 - [2] R. Aaij *et al.* [LHCb Collaboration], *Eur. Phys. J. C* **73**, no. 4, 2373 (2013) doi: 10.1140/epjc/s10052-013-2373-2 [arXiv:1208.3355 [hep-ex]].
 - [3] M. Bauer, B. Stech, M. Wirbel, *Z. Phys. C* **34** (1987) 103 DOI: 10.1007/BF01561122
 - [4] Ahmed Ali, G. Kramer, Cai-Dian Lu, *Phys. Rev. D* **58** (1998) 094009, DOI: 10.1103/PhysRevD.58.094009 [hep-ph/9804363]; *Phys. Rev. D* **59** (1999) 014005 DOI: 10.1103/PhysRevD.59.014005 [hep-ph/9805403]
 - [5] M. Beneke, G. Buchalla, M. Neubert and C. T. Sachrajda, *Nucl. Phys. B* **591**, 313 (2000) doi: 10.1016/S0550-3213(00)00559-9 [hep-ph/0006124].
 - [6] C. D. Lu, K. Ukai and M. Z. Yang, *Phys. Rev. D* **63**, 074009 (2001) doi: 10.1103/PhysRevD.63.074009 [hep-ph/0004213]; Y. Y. Keum, H. N. Li and A. I. Sanda, *Phys. Rev. D* **63**, 054008 (2001) doi: 10.1103/PhysRevD.63.054008 [hep-ph/0004173].
 - [7] C. W. Bauer, S. Fleming, D. Pirjol and I. W. Stewart, *Phys. Rev. D* **63**, 114020 (2001) doi: 10.1103/PhysRevD.63.114020 [hep-ph/0011336].
 - [8] H. Y. Cheng and C. K. Chua, *Phys. Rev. D* **80**, 114008 (2009) doi: 10.1103/PhysRevD.80.114008 [arXiv:0909.5229 [hep-ph]].
 - [9] C. W. Bauer, D. Pirjol, I. Z. Rothstein and I. W. Stewart, *Phys. Rev. D* **70**, 054015 (2004) doi: 10.1103/PhysRevD.70.054015 [hep-ph/0401188].
 - [10] H. n. Li, S. Mishima and A. I. Sanda, *Phys. Rev. D* **72**, 114005 (2005) doi: 10.1103/PhysRevD.72.114005 [hep-ph/0508041].
 - [11] H. n. Li and S. Mishima, *Phys. Rev. D* **90**, no. 7, 074018 (2014) doi: 10.1103/PhysRevD.90.074018 [arXiv:1407.7647 [hep-ph]].
 - [12] Y. K. Hsiao, C. F. Chang and X. G. He, *Phys. Rev. D* **93**, no. 11, 114002 (2016) doi:10.1103/PhysRevD.93.114002 [arXiv:1512.09223 [hep-ph]].
 - [13] C. W. Chiang and Y. F. Zhou, *J. High Energy Phys.* **12** (2006) 027; *J. High Energy Phys.* **03** (2009) 055.

- [14] H. Y. Cheng, C. W. Chiang and A. L. Kuo, Phys. Rev. D **91**, no. 1, 014011 (2015) doi: 10.1103/PhysRevD.91.014011 [arXiv:1409.5026 [hep-ph]].
- [15] H. n. Li, C. D. Lu and F. S. Yu, Phys. Rev. D **86**, 036012 (2012) doi: 10.1103/PhysRevD.86.036012 [arXiv:1203.3120 [hep-ph]].
- [16] H. n. Li, C. D. Lu, Q. Qin and F. S. Yu, Phys. Rev. D **89**, no. 5, 054006 (2014) doi: 10.1103/PhysRevD.89.054006 [arXiv:1305.7021 [hep-ph]].
- [17] Q. Qin, H. N. Li, C. D. Lü and F. S. Yu, Int. J. Mod. Phys. Conf. Ser. **29**, 1460209 (2014). doi:10.1142/S2010194514602099; R. Aaij *et al.* [LHCb Collaboration], Phys. Rev. Lett. **116**, no. 19, 191601 (2016) doi:10.1103/PhysRevLett.116.191601 [arXiv:1602.03160 [hep-ex]].
- [18] S. H. Zhou, Y. B. Wei, Q. Qin, Y. Li, F. S. Yu and C. D. Lu, Phys. Rev. D **92**, no. 9, 094016 (2015) doi: 10.1103/PhysRevD.92.094016 [arXiv:1509.04060 [hep-ph]].
- [19] W. Wang, Y. M. Wang, D. S. Yang and C. D. Lu, Phys. Rev. D **78**, 034011 (2008) doi: 10.1103/PhysRevD.78.034011 [arXiv:0801.3123 [hep-ph]].
- [20] Zhou Rui, Gao Xiangdong and C. D. Lu, Eur. Phys. J. C **72** (2012) 1923 doi:10.1140/epjc/s10052-012-1923-3 [arXiv:1111.0181 [hep-ph]].
- [21] K. A. Olive *et al.* [Particle Data Group Collaboration], Chin. Phys. C **38**, 090001 (2014). doi: 10.1088/1674-1137/38/9/090001
- [22] H. Y. Cheng, C. K. Chua and C. W. Hwang, Phys. Rev. D **69**, 074025 (2004) doi: 10.1103/PhysRevD.69.074025 [hep-ph/0310359].
- [23] P. Ball, G. W. Jones and R. Zwicky, Phys. Rev. D **75**, 054004 (2007) doi: 10.1103/PhysRevD.75.054004 [hep-ph/0612081].
- [24] A. Bharucha, D. M. Straub and R. Zwicky, arXiv:1503.05534 [hep-ph].
- [25] M. Jamin and B. O. Lange, Phys. Rev. D **65**, 056005 (2002) doi: 10.1103/PhysRevD.65.056005
- [26] P. Gelhausen, A. Khodjamirian, A. A. Pivovarov and D. Rosenthal, Phys. Rev. D **88**, 014015 (2013) Erratum: [Phys. Rev. D **89**, 099901 (2014)] Erratum: [Phys. Rev. D **91**, 099901 (2015)] doi: 10.1103/PhysRevD.88.014015, 10.1103/PhysRevD.91.099901, 10.1103/PhysRevD.89.099901 [arXiv:1305.5432 [hep-ph]].
- [27] A. A. Penin and M. Steinhauser, Phys. Rev. D **65**, 054006 (2002) doi: 10.1103/PhysRevD.65.054006 [hep-ph/0108110].
- [28] S. Narison, Phys. Lett. B **520**, 115 (2001) doi: 10.1016/S0370-2693(01)01116-9 [hep-ph/0108242].

- [29] W. Lucha, D. Melikhov and S. Simula, J. Phys. G **38**, 105002 (2011) doi: 10.1088/0954-3899/38/10/105002 [arXiv:1008.2698 [hep-ph]].
- [30] S. Narison, Phys. Lett. B **718**, 1321 (2013) doi: 10.1016/j.physletb.2012.10.057 [arXiv:1209.2023 [hep-ph]].
- [31] R. J. Dowdall *et al.* [HPQCD Collaboration], Phys. Rev. Lett. **110**, no. 22, 222003 (2013) doi: 10.1103/PhysRevLett.110.222003 [arXiv:1302.2644 [hep-lat]].
- [32] N. Carrasco *et al.*, PoS LATTICE **2013**, 313 (2014) [arXiv:1311.2837 [hep-lat]].
- [33] P. Dimopoulos *et al.* [ETM Collaboration], JHEP **1201**, 046 (2012) doi: 10.1007/JHEP01(2012)046 [arXiv:1107.1441 [hep-lat]].
- [34] C. McNeile, C. T. H. Davies, E. Follana, K. Hornbostel and G. P. Lepage, Phys. Rev. D **85**, 031503 (2012) doi: 10.1103/PhysRevD.85.031503 [arXiv:1110.4510 [hep-lat]].
- [35] A. Bazavov *et al.* [Fermilab Lattice and MILC Collaborations], Phys. Rev. D **85**, 114506 (2012) doi: 10.1103/PhysRevD.85.114506 [arXiv:1112.3051 [hep-lat]].
- [36] H. Na, C. J. Monahan, C. T. H. Davies, R. Horgan, G. P. Lepage and J. Shigemitsu, Phys. Rev. D **86**, 034506 (2012) doi: 10.1103/PhysRevD.86.034506 [arXiv:1202.4914 [hep-lat]].
- [37] A. Bussone *et al.*, arXiv:1411.5566 [hep-lat].
- [38] F. Bernardoni *et al.* [ALPHA Collaboration], Phys. Lett. B **735**, 349 (2014) doi: 10.1016/j.physletb.2014.06.051 [arXiv:1404.3590 [hep-lat]].
- [39] D. Melikhov and B. Stech, Phys. Rev. D **62**, 014006 (2000) doi: 10.1103/PhysRevD.62.014006 [hep-ph/0001113].
- [40] C. Q. Geng, C. W. Hwang, C. C. Lih and W. M. Zhang, Phys. Rev. D **64**, 114024 (2001) doi: 10.1103/PhysRevD.64.114024 [hep-ph/0107012].
- [41] C. D. Lu, W. Wang and Z. T. Wei, Phys. Rev. D **76**, 014013 (2007) doi: 10.1103/PhysRevD.76.014013 [hep-ph/0701265 [HEP-PH]].
- [42] C. Albertus, Phys. Rev. D **89**, no. 6, 065042 (2014) doi: 10.1103/PhysRevD.89.065042 [arXiv:1401.1791 [hep-ph]].
- [43] H. Y. Cheng and C. K. Chua, Phys. Rev. D **81**, 114006 (2010) Erratum: [Phys. Rev. D **82**, 059904 (2010)] doi: 10.1103/PhysRevD.81.114006, 10.1103/PhysRevD.82.059904 [arXiv:0909.4627 [hep-ph]].
- [44] C. H. Chen, Y. L. Shen and W. Wang, Phys. Lett. B **686**, 118 (2010) doi: 10.1016/j.physletb.2010.02.056 [arXiv:0911.2875 [hep-ph]].

- [45] P. Ball and V. M. Braun, Phys. Rev. D **58**, 094016 (1998) doi: 10.1103/PhysRevD.58.094016 [hep-ph/9805422].
- [46] P. Ball, JHEP **9809**, 005 (1998) doi: 10.1088/1126-6708/1998/09/005 [hep-ph/9802394].
- [47] P. Ball and R. Zwicky, JHEP **0110**, 019 (2001) doi: 10.1088/1126-6708/2001/10/019 [hep-ph/0110115].
- [48] P. Ball and R. Zwicky, Phys. Rev. D **71**, 014015 (2005) doi: 10.1103/PhysRevD.71.014015 [hep-ph/0406232].
- [49] P. Ball and R. Zwicky, Phys. Rev. D **71**, 014029 (2005) doi: 10.1103/PhysRevD.71.014029 [hep-ph/0412079].
- [50] P. Ball and G. W. Jones, JHEP **0708**, 025 (2007) doi: 10.1088/1126-6708/2007/08/025 [arXiv:0706.3628 [hep-ph]].
- [51] J. Charles, A. Le Yaouanc, L. Oliver, O. Pene and J. C. Raynal, Phys. Rev. D **60**, 014001 (1999) doi: 10.1103/PhysRevD.60.014001 [hep-ph/9812358].
- [52] A. Bharucha, T. Feldmann and M. Wick, JHEP **1009**, 090 (2010) doi: 10.1007/JHEP09(2010)090 [arXiv:1004.3249 [hep-ph]].
- [53] A. Bharucha, JHEP **1205**, 092 (2012) doi: 10.1007/JHEP05(2012)092 [arXiv:1203.1359 [hep-ph]].
- [54] A. Khodjamirian, T. Mannel and N. Offen, Phys. Rev. D **75**, 054013 (2007) doi: 10.1103/PhysRevD.75.054013 [hep-ph/0611193].
- [55] A. Khodjamirian, T. Mannel, N. Offen and Y.-M. Wang, Phys. Rev. D **83**, 094031 (2011) doi: 10.1103/PhysRevD.83.094031 [arXiv:1103.2655 [hep-ph]].
- [56] Y. M. Wang and Y. L. Shen, Nucl. Phys. B **898**, 563 (2015) doi: 10.1016/j.nuclphysb.2015.07.016 [arXiv:1506.00667 [hep-ph]].
- [57] U. G. Meissner and W. Wang, Phys. Lett. B **730**, 336 (2014) doi: 10.1016/j.physletb.2014.02.009 [arXiv:1312.3087 [hep-ph]].
- [58] Y. L. Wu, M. Zhong and Y. B. Zuo, Int. J. Mod. Phys. A **21**, 6125 (2006) doi: 10.1142/S0217751X06033209 [hep-ph/0604007].
- [59] X. G. Wu and T. Huang, Phys. Rev. D **79**, 034013 (2009) doi: 10.1103/PhysRevD.79.034013 [arXiv:0901.2636 [hep-ph]].
- [60] G. Duplancic, A. Khodjamirian, T. Mannel, B. Melic and N. Offen, JHEP **0804**, 014 (2008) doi: 10.1088/1126-6708/2008/04/014 [arXiv:0801.1796 [hep-ph]].

- [61] M. A. Ivanov, J. G. Korner, S. G. Kovalenko, P. Santorelli and G. G. Saidullaeva, Phys. Rev. D **85**, 034004 (2012) doi: 10.1103/PhysRevD.85.034004 [arXiv:1112.3536 [hep-ph]].
- [62] M. Ahmady, R. Campbell, S. Lord and R. Sandapen, Phys. Rev. D **89**, no. 7, 074021 (2014) doi: 10.1103/PhysRevD.89.074021 [arXiv:1401.6707 [hep-ph]].
- [63] H. B. Fu, X. G. Wu and Y. Ma, J. Phys. G **43**, no. 1, 015002 (2016) doi: 10.1088/0954-3899/43/1/015002 [arXiv:1411.6423 [hep-ph]].
- [64] H. n. Li, Y. L. Shen and Y. M. Wang, Phys. Rev. D **85**, 074004 (2012) doi: 10.1103/PhysRevD.85.074004 [arXiv:1201.5066 [hep-ph]].
- [65] W. F. Wang and Z. J. Xiao, Phys. Rev. D **86**, 114025 (2012) doi: 10.1103/PhysRevD.86.114025 [arXiv:1207.0265 [hep-ph]].
- [66] W. F. Wang, Y. Y. Fan, M. Liu and Z. J. Xiao, Phys. Rev. D **87**, no. 9, 097501 (2013) doi: 10.1103/PhysRevD.87.097501 [arXiv:1301.0197].
- [67] Y. Y. Fan, W. F. Wang, S. Cheng and Z. J. Xiao, Chin. Sci. Bull. **59**, 125 (2014) doi: 10.1007/s11434-013-0049-9 [arXiv:1301.6246 [hep-ph]].
- [68] Y. Y. Fan, W. F. Wang and Z. J. Xiao, Phys. Rev. D **89**, no. 1, 014030 (2014) doi: 10.1103/PhysRevD.89.014030 [arXiv:1311.4965 [hep-ph]].
- [69] T. Kurimoto, H. n. Li and A. I. Sanda, Phys. Rev. D **65**, 014007 (2002) doi: 10.1103/PhysRevD.65.014007 [hep-ph/0105003].
- [70] C. D. Lu and M. Z. Yang, Eur. Phys. J. C **28**, 515 (2003) doi: 10.1140/epjc/s2003-01199-y [hep-ph/0212373].
- [71] Z. T. Wei and M. Z. Yang, Nucl. Phys. B **642**, 263 (2002) doi: 10.1016/S0550-3213(02)00623-5 [hep-ph/0202018].
- [72] T. Huang and X. G. Wu, Phys. Rev. D **71**, 034018 (2005) doi: 10.1103/PhysRevD.71.034018 [hep-ph/0412417].
- [73] R. R. Horgan, Z. Liu, S. Meinel and M. Wingate, Phys. Rev. D **89**, no. 9, 094501 (2014) doi: 10.1103/PhysRevD.89.094501 [arXiv:1310.3722 [hep-lat]].
- [74] E. Dalgic, A. Gray, M. Wingate, C. T. H. Davies, G. P. Lepage and J. Shigemitsu, Phys. Rev. D **73**, 074502 (2006) Erratum: [Phys. Rev. D **75**, 119906 (2007)] doi: 10.1103/PhysRevD.75.119906, 10.1103/PhysRevD.73.074502 [hep-lat/0601021].
- [75] S. Aoki *et al.*, Eur. Phys. J. C **74**, 2890 (2014) doi: 10.1140/epjc/s10052-014-2890-7 [arXiv:1310.8555 [hep-lat]].

- [76] F. Ambrosino *et al.*, JHEP **0907**, 105 (2009) doi: 10.1088/1126-6708/2009/07/105 [arXiv:0906.3819 [hep-ph]].
- [77] T. Feldmann, P. Kroll and B. Stech, Phys. Rev. D **58**, 114006 (1998) doi: 10.1103/PhysRevD.58.114006 [hep-ph/9802409].
- [78] T. Feldmann, P. Kroll and B. Stech, Phys. Lett. B **449**, 339 (1999) doi: 10.1016/S0370-2693(99)00085-4 [hep-ph/9812269].
- [79] F. James and M. Winker. *http : www.cern.ch/minuit*. CERN, May 2004.
- [80] Y. Li, C. D. Lu, Z. J. Xiao and X. Q. Yu, Phys. Rev. D **70** (2004) 034009 doi: 10.1103/PhysRevD.70.034009 [hep-ph/0404028]; A. Ali, G. Kramer, Y. Li, C. D. Lu, Y. L. Shen, W. Wang and Y. M. Wang, Phys. Rev. D **76** (2007) 074018 doi: 10.1103/PhysRevD.76.074018 [hep-ph/0703162 [HEP-PH]]; Z.J. Xiao, W.F. Wang and Y.Y. Fan, Phys. Rev. D **85** (2012) 094003 doi:10.1103/PhysRevD.85.094003 [arXiv:1111.6264 [hep-ph]].